

# High-(Energy)-Lights

## The Very High Energy Gamma-Ray Sky

Dieter Horns

Institute for Experimental Physics, University of Hamburg  
Luruper Chaussee 149, D-22761 Hamburg  
dieter.horns@desy.de

### Abstract

*The high-lights of ground-based very-high-energy (VHE,  $E > 100$  GeV) gamma-ray astronomy are reviewed. The summary covers both Galactic and extragalactic sources. Implications for our understanding of the non-thermal Universe are discussed. Identified VHE sources include various types of supernova remnants (shell-type, mixed morphology, composite) including pulsar wind nebulae, and X-ray binary systems. A diverse population of VHE-emitting Galactic sources include regions of active star formation (young stellar associations), and massive molecular clouds. Different types of active galactic nuclei have been found to emit VHE gamma-rays: besides predominantly Blazar-type objects, a radio-galaxy and a flat-spectrum radio-quasar have been discovered. Finally, many (presumably Galactic) sources have no convincing counterpart and remain at this point unidentified. A total of at least 70 sources are currently known. The next generation of ground based gamma-ray instruments aims to cover the entire accessible energy range from as low as  $\approx 10$  GeV up to  $10^5$  GeV and to improve the sensitivity by an order of magnitude in comparison with current instruments.*

## 1 Introduction

The highest energy photons known are produced in astrophysical processes involving even more energetic particles presumably accelerated through stochastic acceleration mechanisms as suggested initially by Fermi (1949). Therefore, observations of VHE photons provide a direct view of the astrophysical accelerators of charged particles and allow to identify the individual sources of cosmic rays: VHE photons open our view to the “accelerator sky”. The origin of the Galactic population of charged cosmic rays has remained since its discovery by V. Hess in 1912 until today a long-standing question of astro- and particle physics. A widely favored model on the origin of cosmic rays assumes that diffusive shock acceleration takes place in the expanding blast waves of supernova remnants converting 10–20 % of the kinetic energy into cosmic rays. Under this assumption, Galactic supernova remnants provide sufficient power ( $\approx 10^{41}$  ergs  $s^{-1}$ ) in order to balance the escape losses of Galactic cosmic rays as well as produce a power-law type distribution of particle energy that closely resembles the cosmic ray spectrum measured locally (see e.g. Ginzburg & Syrovatskii 1964; Hillas 2006).

Observations of VHE-gamma-rays, mainly by imaging air Cherenkov telescopes in the last decade, have surpassed the anticipated detection of a few supernova remnants and have established a rich and diverse collection of VHE sources. Specifically, the currently active generation of imaging air Cherenkov telescopes (H.E.S.S.<sup>1</sup>, MAGIC<sup>2</sup>, and VERITAS<sup>3</sup>) have fulfilled and by far exceeded the expectations that were based upon the pioneering previous generation of experiments: the results obtained in the last years have shown that VHE emission is common to a variety of different source types - not only shell-type SNRs.

The current view of the source distribution in the VHE sky is shown in Figure 1 where all known sources are displayed (status of September 2008). Note, the sensitivity achieved varies greatly across the sky. The best sensitivity is reached in the inner Galactic disk where a dedicated survey with the air Cherenkov telescopes of the H.E.S.S. experiment has been performed (see section 2.2).

The most remarkable feature of the gamma-ray sky is not evident in this picture: each source shown is an accelerator of particles up to and beyond TeV energies (“accelerator sky”). A similar conclusion can not be drawn when looking at source populations detected in other wavelength bands. This makes the VHE band a sensitive window to detect non-thermal particle accelerators. Future neutrino telescopes will almost certainly have the potential to detect some of the brighter VHE sources (and discover new sources that are optically thick for VHE gamma-rays). The detection of high energy neutrinos is experimentally a challenging task and requires tremendous efforts (see e.g. the Ice-CUBE neutrino telescope in the Antarctic ice). However, the observation of a neutrino source will ultimately demonstrate the presence of accelerated nuclei - largely model-independent. Different to the clear observational signature in the neutrino channel, VHE gamma-rays are sensitive to accelerated electrons (through inverse Compton scattering) as well as to accelerated nuclei (through neutral meson production and decay).

The scope of this article is limited to observational highlights obtained with ground based instruments and does not aim at presenting a complete review of the field of VHE astrophysics. The paper is structured in the following way: In section 2, the experimental techniques of ground-based instruments (both imaging and non-imaging) are described before continuing with the census of today’s VHE sky in section 3. Section 4 provides a short overview on VHE gamma-rays as probes of the interstellar medium including Lorenz-invariance violating effects related to structure of space-time at Planck-scales. Finally, in section 5 this review is concluded with some comments on the future of the field.

## 2 Observational techniques

Non-thermal gamma-ray sources produce typically power-law type energy spectra in which the flux drops with increasing energy. As a consequence of this, space based detection techniques are limited by the small detection rate of photons at high ener-

---

<sup>1</sup><http://www.mpi-hd.mpg.de/hfm/HESS/HESS.html>

<sup>2</sup><http://www.magic.mppmu.mpg.de/>

<sup>3</sup><http://veritas.sao.arizona.edu/>

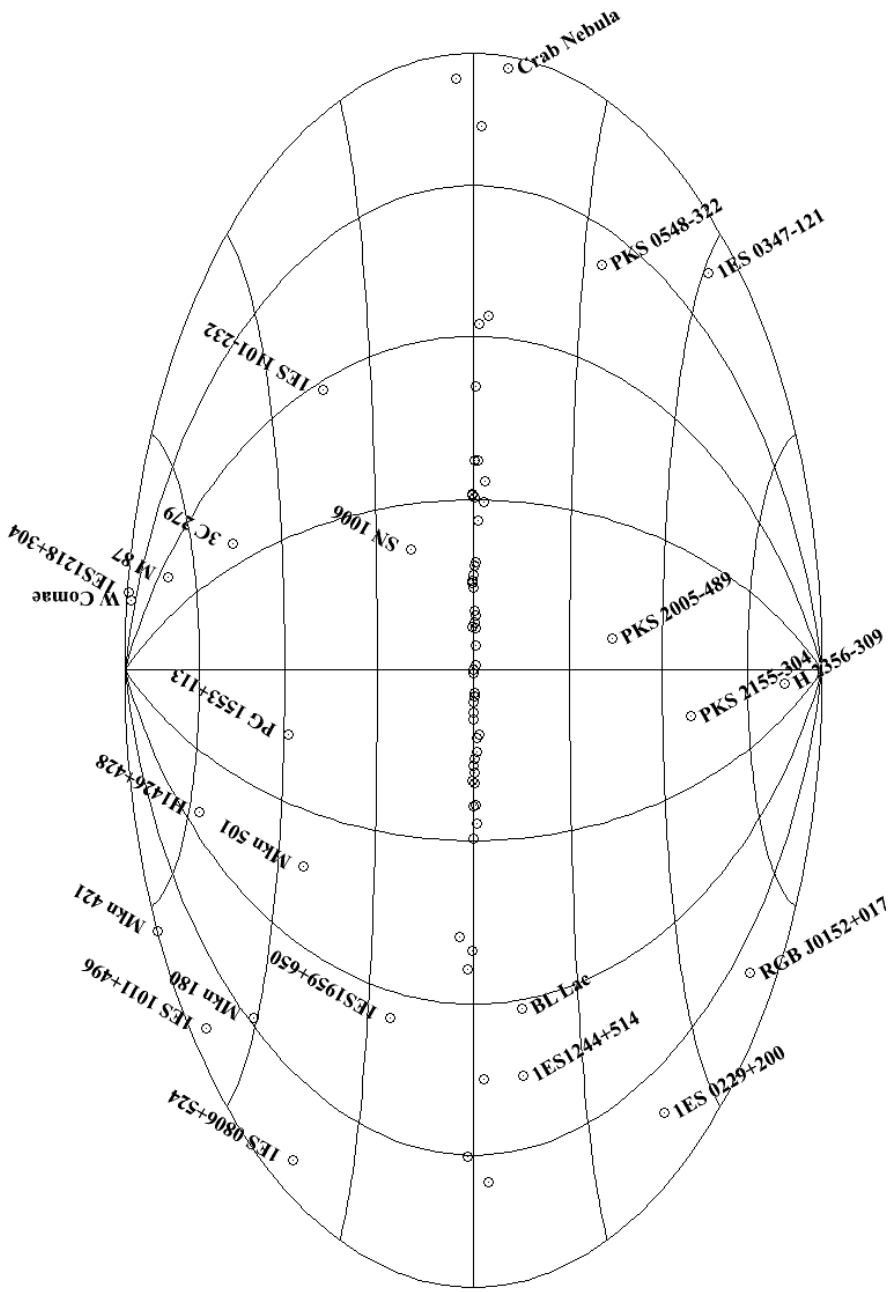


Figure 1: All VHE sources as known in September 2008 are shown as circles in a Hammer-Aitoff projection of a Galactic coordinate system. The Galactic center is in the center of the picture.

gies ( $E < 10 - 100$  GeV). The detection of VHE ( $E > 100$  GeV) photons requires collection areas that are substantially larger than the  $\mathcal{O}(\text{m}^2)$  of satellite based detectors. One approach towards large collection areas are ground based observation techniques which however are limited to energies sufficiently high ( $E > 5$  GeV) to produce a detectable air shower.

Ground based gamma-ray observations are always based upon air shower detection techniques. High energy particles (photons, electrons, and nuclei) initiate extensive air showers in the atmosphere which acts as a natural calorimeter: secondary particles are detected either when they reach the ground or by the Cherenkov light produced in the atmosphere. At ultra-high energies, it becomes feasible to detect fluorescence light as well as radio signals which are not discussed here (see e.g. the contribution by J. Hörandel at this conference).

Generally, the air shower detection technique relies on one of the following approaches:

- Shower-front sampling of particles
- Shower-front sampling of Cherenkov light
- Imaging of the air shower using Cherenkov light.

The benefits (marked '+' ) and draw-backs ('-') of the shower-front sampling of particles and the imaging air Cherenkov technique are mainly the following<sup>4</sup>:

- Imaging technique:
  - + sensitivity ( $\approx 10^{-13}$  ergs/(cm<sup>2</sup> s)<sup>-1</sup> at TeV-energies, 50 hrs exposure)
  - + angular resolution (few arc minutes per event)
  - + spectroscopy ( $\Delta E/E \approx 15$  %)
  - + low energy threshold
  - field of view (a few degrees,  $\approx$  msrad)
  - duty cycle ( $\approx 10$  %)
- Shower front sampling of particles:
  - + high duty cycle ( $\approx 95$  %)
  - + large field of view ( $\approx 2$  srad)
  - high energy threshold
  - sensitivity ( $\approx 10^{-12}$  ergs cm<sup>-2</sup> s<sup>-1</sup>, 1 year exposure)
  - angular resolution ( $0.3 - 0.7^\circ$ )
  - energy resolution ( $\Delta E/E \approx 30 - 100$  %)

---

<sup>4</sup>Shower-front sampling of Cherenkov light is discussed seperately below.

The obvious complementarity of the two techniques justifies the further development of both of them in the future: non-imaging techniques cover simultaneously a large field of view and can be operated 24 hours a day. On the other hand, air Cherenkov telescopes have a narrow field of view (a few milli steradians), reaching a supreme sensitivity, but can only be operated in clear, dark nights.

In addition to the indirect ground based techniques discussed until now, high energy gamma-rays can be detected above the atmosphere directly by pair-conversion detectors. With these detectors, events initiated by charged particles can be effectively suppressed by e.g. a scintillation veto shield. Obviously, this is not possible for ground based indirect detection techniques where a separation of gamma-ray and cosmic-ray events has to be done using the information of the air shower itself (gamma-hadron separation).

With the commissioning of the Fermi satellite<sup>5</sup> (Atwood et al. 2007), ground-based gamma-ray astronomy will benefit from the simultaneous operation of essentially a sensitive all-sky monitor operating at lower energies. The sensitivity of Fermi is well matched by the sensitivity of ground-based experiments so that the two instruments will be able to provide detection or constraints on the spectral shape across 6-7 orders of magnitude in energy.

## 2.1 Shower-front sampling techniques

**Particle arrays.** The experimental approach for the measurement of cosmic rays as well as the search for gamma-ray sources had been largely dominated by air shower arrays until the beginning of the 1990's. These arrays of particle detectors measure the arrival time of the shower front and the lateral particle density distribution. The total number of particles in the air shower is used to reconstruct the total energy of the primary particle. The relative timing of the individual particle detectors in the array is used to determine the direction of the air shower (typical angular resolutions of  $1^\circ$  can be reached) while both the timing and particle density measured on the ground are in principle useful to discern electromagnetic from hadronic air-showers (gamma-hadron separation). However, the gamma-hadron separation is naturally limited by the filling factor<sup>6</sup> of the detector array which typically amounts to less than 1%. An important development in the field was the innovation introduced by the MILAGRO collaboration (see e.g. Atkins et al. 2004): they use a pond of water which is instrumented with photo-multiplier tubes (PMTs). The PMTs detect Cherenkov light from the secondary particles entering the pond's water. This way, the filling factor is increased to almost 100% and the entire particle distribution is sampled by the detector. Using the *clumpiness* of the particle distribution as an indicator for a hadronic air shower<sup>7</sup>, it has been possible to reach sufficient sensitivities to detect VHE gamma-ray sources.

Future projects along this direction aim at installing such a detector at high altitude, where the energy threshold can be decreased to reach values below 1 TeV. Parallel

---

<sup>5</sup>formerly known as GLAST

<sup>6</sup>the fraction of the total surface covered with active detector surface

<sup>7</sup>for electromagnetic air showers, the lateral distribution is smoother than for a hadronic shower which contains muons and sub-showers

to the MILAGRO group, the ARGO collaboration has developed a new type of air shower detector using resistive plate chambers to increase the filling factor. Their installation is already located at high altitude and is starting operation (Aielli & The Argo-YBJ Collaboration 2007). For a review of ground based non-imaging detectors, see Lorenz (2007).

**Shower-front sampling with Cherenkov light.** The experimental technique used by non-imaging air Cherenkov detectors marks the transition from non-imaging to imaging observations. These detectors sample the arrival time and density of air Cherenkov photons using either open PMTs like e.g. the THEMISTOCLE experiment (Fontaine et al. 1990), AIROBICC array (Karle et al. 1995) or large reflecting surfaces as e.g. heliostats provided by solar power plants. The latter approach has been pursued by a number of groups including the C.A.C.T.U.S. (Marleau et al. 2005), CELESTE (Paré et al. 2002) as well as STACEE (D. M. Gingrich et al. 2005). While arrays of open PMTs retain the large field of view of classical air shower sampling arrays, the heliostat arrays have a very small field of view but a substantially smaller energy threshold reaching below 100 GeV as achieved e.g. by the CELESTE experiment. The potential for discovering faint sources is limited by the gamma-hadron rejection power of these shower sampling instruments.

## 2.2 Imaging air Cherenkov telescopes

The field of ground-based gamma astronomy has been largely driven by the remarkable results obtained with the imaging air Cherenkov telescopes (IACTs). Extensive air showers emit in the forward-direction a beam of atmospheric Cherenkov light with an opening angle of  $\approx 1^\circ$ . This beam illuminates almost homogeneously a circular region on the ground with a diameter of 200-300 m (depending on the altitude and inclination of the shower axis). An optical telescope pointing parallel to the shower axis and located within the illuminated footprint of the shower can make an image of the air shower against the background light of the night sky, provided the camera is sufficiently fast to integrate the short Cherenkov flash of only a few nanoseconds. The image provides information on the original particle's energy, direction, and on its nature (nucleus or photon). The reconstruction of these parameters is improved considerably when more than one telescope is used in a stereoscopic set-up where the telescopes are separated by 50-150 m in order to provide a baseline for triangulating the atmospheric air shower. The stereoscopic technique has become the nominal standard for all current and future installations.

The performance of today's telescopes is essentially characterized by the sensitivity to detect VHE sources with an energy flux down to  $10^{-13}$  ergs  $(\text{cm}^2 \text{ s})^{-1}$  in 50 hrs of observation time; this corresponds to a minimum detectable luminosity of  $L_{\min} \approx 10^{31}$  ergs  $\text{s}^{-1} (d/1 \text{ kpc})^2$  at a distance of 1 kpc or more suitable for extragalactic objects  $L_{\min} \approx 10^{41}$  ergs  $\text{s}^{-1} (d/100 \text{ Mpc})^2$  at a distance of 100 Mpc.

The angular resolution of each reconstructed primary  $\gamma$ -ray is typically better than 6 arc min. The relative energy resolution is comparably good and reaches values of  $\Delta E/E \approx 10 - 20 \%$ . This is sufficient to detect and characterize spectral features like

curvature or even lines from e.g. self-annihilation of Dark matter particles. For a list of currently operating IACTs see e.g. Hinton (2007).

### 3 A census of today's VHE gamma-ray sky

The currently known list of VHE sources encompasses more than 70 sources (see Fig. 1). The number of sources is modest in comparison with catalogues assembled at lower energies. However, it is remarkable, how many different types of objects are actually emitting VHE gamma-rays and are therefore accelerators of multi-TeV particles.

Before discussing the different source types that have been detected, it is enlightening to list promising source types which have not been detected in the VHE band so far (the possible reason(s) for non-detection listed in parenthesis):

- **Star burst galaxies (too faint):** The high star forming rate should lead ultimately to an enhanced rate of supernova explosions. The upper limits on VHE emission from e.g. NGC 253 (Aharonian et al. 2005h) are still higher than the expected flux (Domingo-Santamaría & Torres 2005) but deeper observations (ca. 50 hrs) will eventually reach the required sensitivity to either detect a signal or put meaningful constraints on the models<sup>8</sup>.
- **Gamma-ray bursts (too short, too far):** These extremely powerful explosions are transient events requiring fast turn-around times and/or wide-field-of-view instruments in order to capture these objects during their outbursts. No convincing GRB detection has been claimed so far.<sup>9</sup> The ultra-fast slewing MAGIC telescope has succeeded in observing (but not detecting) a GRB while the outburst was still ongoing (Albert et al. 2006c). Non-imaging all-sky survey instruments like MILAGRO are probably more likely to detect these transient events including also the distinct class of short GRBs (for constraints see e.g. Abdo et al. 2007c). The visibility of distant GRB events is limited due to absorption of the energetic photons emitted at cosmological distances in pair-production processes with the optical-to-infra-red background light. An energy threshold well below 100 GeV is crucial to be able to observe GRBs at red-shifts  $z > 0.1$ .
- **Clusters of galaxies (too extended, too faint):** So far, no group or cluster of galaxies has been detected in the VHE band. Clusters of galaxies confine effectively cosmic rays and are expected to produce VHE-emission via inelastic scattering of nuclei with the intra-cluster gas (Völk et al. 1996; Pfrommer & Enßlin 2004). In addition to cosmic rays injected by normal galaxies and accelerated in large-scale shocks, AGN activity could also lead to an additional contribution to the intra-cluster cosmic ray density (Hinton et al. 2007b).

---

<sup>8</sup>The CANGAROO collaboration published a claim for a detection from the starburst galaxy NGC 253 which was however later retracted (Itoh et al. 2007).

<sup>9</sup>Some evidence for GRB detections have been published in the past (see e.g. Padilla et al. 1998; Atkins et al. 2000).

Current upper limits do not constrain severely the non-thermal population of cosmic rays in the clusters (Domainko et al. 2007).

- **Pulsars (early cut-off in energy spectrum):** Fast rotating neutron stars are expected to give rise to acceleration within the magnetosphere (for a review, see e.g. Kaspi et al. 2006). This leads to pulsed emission (mainly from curvature radiation) that has been detected at least from six isolated pulsars up to GeV energies with the EGRET spark chamber detector on board the Compton Gamma-Ray Observatory (Thompson et al. 1999). However, the energy spectra of pulsars are also expected to show a sudden cut-off at a few GeV which has made them so far invisible to ground-based telescopes with an energy threshold around 100 GeV. Most searches for pulsed emission above 100 GeV have so-far not been successful in finding VHE emission from pulsars - consistent with the expectations (Aharonian et al. 2007g; Albert et al. 2007b). The MAGIC collaboration has recently reported the first detection of pulsed emission with ground based instruments above 25 GeV at the level of  $6.4 \sigma$  (Teshima 2008). Additionally, pulsed emission has been suggested to be produced via bulk Compton-scattering processes in the un-shocked pulsar wind-zone (Bogovalov & Aharonian 2000). Non-detection of pulsed emission from the Crab pulsar has been used to constrain the formation region of the ultra-relativistic wind (Aharonian et al. 2004a).

The breakdown of known VHE sources includes 50 Galactic objects: 5 shell-type SNRs, 2 mixed-morphology SNRs, 2 composite SNRs, 20 pulsar-wind nebulae, 2 stellar associations, 4 X-ray binary systems, and roughly 18 sources without clear association to known objects. The remaining 23 objects are of extra-galactic origin: 21 Blazars, one Fanaroff-Riley Type I (M 87), and one flat-spectrum radio quasar (3C279).

### 3.1 Shell-type supernova remnants

Shell-type supernova remnants are commonly considered to be the best candidates to accelerate Galactic cosmic rays. During the supernova explosion (either a thermonuclear explosion or a core-collapse event), the stellar atmosphere is ejected with an initial velocity of a few  $1000 \text{ km s}^{-1}$  carrying  $10^{51}$  erg in kinetic energy and driving a shock front in the interstellar medium. While slowing down during the Sedov phase<sup>10</sup>, the expanding shock front heats up the ambient medium giving rise to thermal X-ray emission. The shock is expected to dissipate a good fraction (10 – 30 %) of its energy during the Sedov phase in the form of accelerated particles (electrons and nuclei). In this case, the total power injected by roughly 1 supernova explosion every 30 years is sufficient to balance the escape losses of Galactic cosmic rays. Radio- as well as X-ray synchrotron emission is detected and attributed to electrons accelerated by the forward shock which in projection produces the characteristic shell-like morphology. For a few objects, the non-thermal X-ray component dominates entirely the observed X-ray spectrum (e.g. SN 1006, RX J1713.7-3946).

<sup>10</sup>once the SNR has swept up a comparable amount of matter from the interstellar medium as its ejecta mass, the free expansion phase ends and the Sedov phase of SNR evolution starts



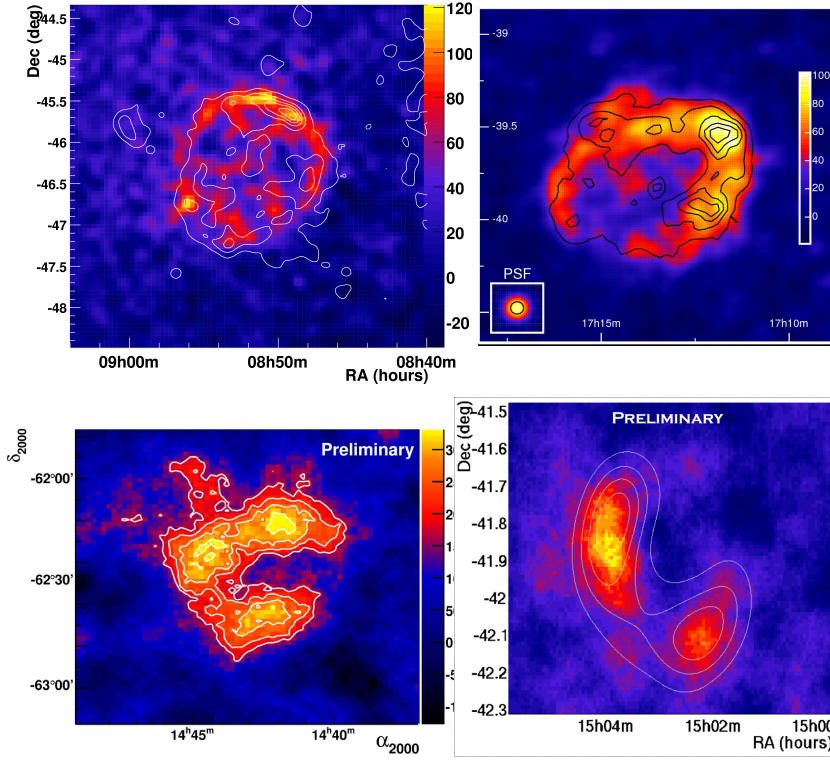


Figure 2: Upper panel, from left to right: RX J0852.0-4622 ("Vela Jr") (Aharonian et al. 2007f), RX J1713.7-3946 (Aharonian et al. 2006d), bottom panel: RCW 86 (Hoppe et al. 2007), SN1006 (Naumann-Godó & H.E.S.S. Collaboration 2008). The color-coded images are the excess maps as obtained with the H.E.S.S. telescopes (see text for references). Overlaid in white contours (RX J0852.0-4622) is the smoothed ROSAT image obtained above 1.3 keV. The black contours overlaid on the VHE-image of RX J1713.7-3946 follow the ASCA image (1-3 keV). The white contours overlaid on RCW 86 are the significance contours (starting at 3 standard deviations, increasing by 1) The white contours on the preliminary excess map from SN 1006 follows the Chandra X-ray map smoothed to match the H.E.S.S. point-spread function.

However, radio and X-ray observations are sensitive mainly to electrons and only indirectly to the presence of energetic nuclei: X-ray observations with sub-arcsecond spatial resolution have revealed indirectly, that the forward shock in many SNRs is very likely modified by cosmic ray streaming instabilities leading to enhanced magnetic field compression (Lucek & Bell 2000). This in turn leads to observable effects: electrons produce X-ray synchrotron emission in small regions with increased magnetic field upstream of the shock that appear as narrow X-ray filaments ( $d < 1$  pc) that have been first detected using the superior angular resolution of the Chandra X-ray telescope (Bamba et al. 2003). The inferred magnetic field strength in the X-ray filaments of e.g. SN1006 is of the order of  $100 \mu\text{G}$  (Berezhko et al. 2003) which is much larger than in the case of a linear shock thus indirectly revealing efficient acceleration of nuclei. Recent observations of fast variability of X-ray emission in filamentary structures seems to provide additional evidence for strong magnetic fields in RX J1713.7-3946 (Uchiyama et al. 2007).

VHE gamma-ray observations are sensitive to both, electrons as well as nuclei. Sufficiently energetic electrons can radiate VHE gamma-rays through inverse Compton-up-scattering of soft seed photons (leptonic origin of VHE-emission) while nuclei produce neutral mesons decaying into gamma-rays in inelastic scattering events with the ambient gas (hadronic origin of VHE-emission).

In the hadronic scenario, the energy loss-time for accelerated protons ( $\tau_{pp \rightarrow \pi^0} \approx 4.5 \times 10^{15} n^{-1}$  s) varies only slowly with energy and depends mainly on the ambient medium density ( $n_H = n \text{ cm}^{-3}$ ) which includes cold molecular and hot ionized gas as well as the ejecta of the progenitor star. The actual density of gas near the shock can be inferred e.g. by modeling thermal X-ray emission from heated and partially ionized gas. However, for SNR without thermal X-rays, the density can only be constrained rather loosely and uncertainties close to an order of magnitude can remain. The typical integrated luminosity in VHE gamma-rays (1-10 TeV) is from a population of energetic protons with total energy  $W_p$   $L_\gamma \approx W_p \tau^{-1} = 3.7 \cdot 10^{33} \cdot \eta / 0.1 \cdot (E_{\text{SN}} / 10^{51} \text{ ergs}) n \text{ ergs s}^{-1}$  for an efficiency of shock acceleration  $\eta = 0.1$ , ie. the fraction of the kinetic energy of the blast wave converted into charged particles accelerated<sup>11</sup>. A similar result on the SNR luminosity has been obtained by Drury et al. (1994).

Currently four VHE-emitting shell-type SNRs are detected and upper limits have been derived for a few more objects (see Table 1 for a list). Except for Cassiopeia A, the spatial extension of the SNR has been resolved (see Fig. 2). Generally, the observed luminosities of the shell-type SNRs are consistent with the expected luminosity in the hadronic scenario. For RX J0852.0-4622 (Vela Jr.), the distance estimates are controversial and therefore the luminosity uncertainties can be as large as 2 orders of magnitude. See the references given in Table 1 for more details. Within this uncertainty on the distance of Vela Jr., the VHE observations are consistent with the indirect evidence from X-ray observations for efficient shock acceleration of nuclei. A leptonic origin can not be excluded but is disfavored as it would lead to a comparably small efficiency for acceleration of nuclei which in turn would not produce non-linear modifications as are observed in X-rays. For Cassiopeia A, the average

---

<sup>11</sup>The accelerated spectrum is assumed to follow a power-law with  $dn/dE \propto E^{-2}$

magnetic field is known to be larger than  $80 \mu\text{G}$  Cowsik & Sarkar (1980) and may be as large as  $1 \mu\text{G}$  if magnetic field and particle energy density are in equipartition. This implies that the corresponding particle number density and the expected inverse Compton flux is too small to explain the observed VHE emission which effectively rules out a leptonic origin of the observed VHE emission in this particular case.

A second crucial test of the SNR origin of cosmic rays is the spectral shape and maximum energy of particles accelerated<sup>12</sup>. The observed VHE energy spectra from RX J1713.7-3946 (Aharonian et al. 2006d) and RX J0852.0-4622 (Aharonian et al. 2007f) indicate that the accelerated proton spectrum follows an  $E_p^{-2}$  type power-law and cuts off at energies of roughly 100-200 TeV which is about one order of magnitude smaller than the energy of the “knee” in the cosmic ray all-particle spectrum at a few  $10^{15}$  eV. This discrepancy can be accommodated if these two SNRs are already too old and the shock has decelerated such that the maximum energy has dropped to the currently observed value (Ptuskin & Zirakashvili 2005) while the more energetic particles have already escaped the remnant.

In this context, the young SNR Cassiopeia A<sup>13</sup> and its VHE properties are crucial to our understanding of the SNR contribution to cosmic rays. Cassiopeia A has been confirmed by the MAGIC and VERITAS collaborations to be a VHE-emitting source (Albert et al. 2007f; Humensky & VERITAAS Collaboration 2008) after the initial discovery with HEGRA (Aharonian et al. 2001a). The available spectra measured with HEGRA and MAGIC are in agreement with each other but require a rather soft energy spectrum with a photon index close to 2.5. The total energy in protons  $W_p \approx 2 \times 10^{49}$  ergs is only a small fraction of the kinetic energy of the blast wave and only a factor of 4-8 larger than the inferred energy in accelerated electrons (Atoyan et al. 2000). Given the young age of the source which is at the beginning of the Sedov phase, the small value of  $W_p$  may still be re-reconciled with Cassiopeia A to be a typical SNR. It will be quite interesting to measure with better accuracy the energy spectrum to higher energies in order to probe the maximum energy of accelerated protons which should be close to PeV energies. Furthermore, as indicated in Table 1, future detections (or stronger constraints) of VHE-emission from other historical SNRs like Tycho or Kepler will provide important clues on cosmic-ray acceleration in these objects.

### 3.2 Mixed morphology supernova remnants

Besides young ( $t \approx \mathcal{O}(1000)$  yrs) shell-type supernova-remnants, VHE-gamma-ray emission has also been detected from the direction of mixed-morphology (MM) type supernova-remnants (SNRs) which are considered evolved systems. MM systems are characterized by a shell-like emission observed *only* in the radio-band with thermal, centrally-peaked X-ray emission predominantly from the interior of the SNR (see e.g Rho & Petre 1998). The mechanism responsible for heating the gas is not well-understood. It has been suggested that mixed morphology SNR have entered a post-Sedov stage of their evolution which is characterized by an equal electron and ion temperature (Kawasaki et al. 2005). The fact that roughly 20 % of the known

<sup>12</sup>which can not be inferred from observations in other wavelengths

<sup>13</sup>and also Vela Jr if the age is in the range of 200-300 yrs

Table 1: List of supernova-remnants (shell-type and mixed-morphology) observed in VHE gamma-rays .

Name	distance [kpc]	$L_\gamma$ [ $10^{33}$ ergs/s]	age [kyrs]	Type
Cas A	3.4 <sup>a</sup>	1.4 <sup>b</sup>	0.33 <sup>c</sup>	Shell, II
RX J1713.7-3946	$\simeq 1$ <sup>d</sup>	5.7 <sup>E</sup>	1.6 <sup>e</sup>	Shell, II/Ib <sup>f</sup>
Vela Jr	0.2 <sup>g</sup>	0.3 <sup>G</sup>	0.7 <sup>g</sup>	Shell, II
	0.33 <sup>h</sup>	0.6 <sup>G</sup>	0.66 <sup>h</sup>	
	1 – 2 <sup>i</sup>	6-26 <sup>G</sup>	4-19 <sup>i</sup>	
RCW 86	2.8 <sup>j</sup>	5.5 <sup>k</sup>	1.8 (SN185?) <sup>j</sup>	Shell, ?
SN 1006	2.2 <sup>l</sup>	1.4 <sup>L</sup>	1	Shell, Ia
W28	1.9 <sup>l</sup>	0.5 <sup>m</sup>	33 <sup>m</sup>	MM
IC443	1.5 <sup>n</sup>	0.4 <sup>o</sup>	20 <sup>p</sup>	MM
Without detection (historical SNe)				
Tycho	2.2 <sup>q</sup>	< 0.5 <sup>r</sup>	0.4	Shell, Ia
	4.5 <sup>s</sup>	< 2 <sup>r</sup>	(SN1572)	
Kepler	4.8 <sup>u</sup>	< 2.4 <sup>v</sup>	0.4	Shell, Ia <sup>w</sup>
	6.4 <sup>u</sup>	< 4.2 <sup>v</sup>	(SN1604)	

<sup>a</sup>Reed et al. (1995), <sup>b</sup>Aharonian et al. (2001a)(Albert et al. 2007f), <sup>c</sup>Thorstensen et al. (2001), <sup>d</sup>Koyama et al. (1997), <sup>E</sup>Aharonian et al. (2006d), <sup>e</sup>Koyama et al. (1997), <sup>f</sup>Cassam-Chenaï et al. (2004), <sup>G</sup>Aharonian et al. (2007f), <sup>g</sup>Aschenbach et al. (1999), <sup>h</sup>Bamba et al. (2005), <sup>i</sup>Slane et al. (2001), <sup>j</sup>Vink et al. (2006), <sup>k</sup>Hoppe et al. (2007), <sup>L</sup>Naumann-Godó & H.E.S.S. Collaboration (2008), <sup>l</sup>Velázquez et al. (2002), <sup>m</sup>Aharonian et al. (2008e), <sup>n</sup>Claussen et al. (1997), <sup>o</sup>Albert et al. (2007c), <sup>p</sup>Lee et al. (2008), <sup>q</sup>Albinson et al. (1986), <sup>r</sup>Aharonian et al. (2001b), <sup>s</sup>Schwarz et al. (1995), <sup>t</sup>Winkler et al. (2003), <sup>u</sup>Reynoso & Goss (1999), <sup>v</sup>Aharonian et al. (2008b), <sup>w</sup>Reynolds et al. (2007)

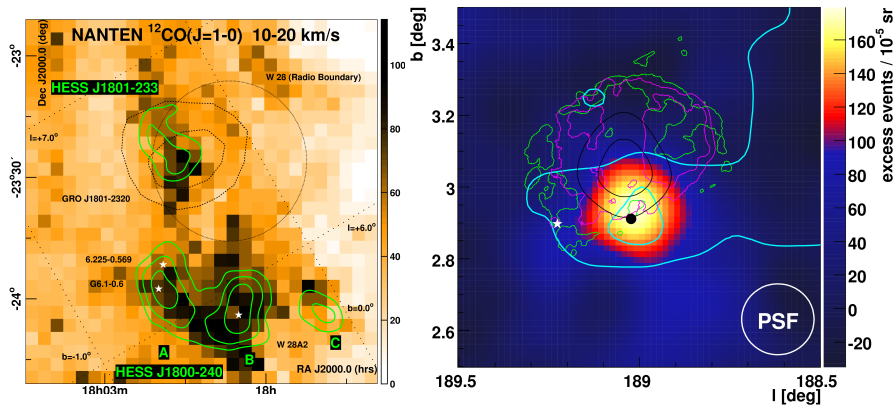


Figure 3: Left panel (a): The integrated CO emission in the velocity range 10-20 km/s (color scale) with significance contours from H.E.S.S. observations of W28 overlaid (green). The black contours follow the 95 % and 99 % confidence level regions for the unidentified EGRET source GRO J1601-2320 (Aharonian et al. 2008e). Right panel (b): The color scale indicates the smoothed excess map obtained from MAGIC observations of IC 443. The molecular gas density (CO) is traced with the cyan colored contours, X-ray contours (purple) from ROSAT observations, gamma-ray contours (EGRET) in black. See captions of Fig. 1 in Albert et al. (2007c) for references.

Galactic SNR are of MM supports this scenario. The observation of VHE gamma-rays from MM SNR like W28 (Aharonian et al. 2008e) and IC443 (Albert et al. 2007c) is – independent of the underlying radiation mechanism – direct evidence for particle acceleration to multi-TeV energies in these objects (see Fig. 3). However, one would expect that the evolved and slow shock present in these objects is not strong enough to accelerate particles at the current stage of evolution. Furthermore, the observed Gamma-ray emission seems to coincide well with regions of dense molecular gas. In the north-eastern region of W28, some of the clouds must have already been interacting with the expanding blast wave. The interaction can be traced by maser emission in the shocked gas (see Fig. 3a). The observation of VHE-emission from IC 443, another MM type SNR, supports a similar scenario of an evolved SNR interacting with dense and cold molecular gas (see Fig. 3b). In this scenario, electrons can not produce the observed VHE-emission because of the rapid cooling through inverse Compton and synchrotron emission, as well as Bremsstrahlung in the dense gas. Typical cooling times of electrons at multi-TeV energies would be of the order of a few hundred years and by far too short to allow for a sizeable population of electrons to be present in an evolved SNR without ongoing acceleration. An alternative and much more favorable interpretation for MM SNRs requires that accelerated nuclei have been partially confined to the SNR and its environment and produce efficiently gamma-rays through  $\pi^0$ -decay in the dense target material of the molecular clouds. Gabici & Aharonian (2007) have

investigated the effect of cosmic rays that have left the accelerator and produce an observable VHE emission in a nearby cloud of molecular gas.

### 3.3 Pulsar wind nebulae and composite supernova remnants

While shell type SNR are considered to be the likely source of the Galactic cosmic rays, the blind survey of the Galactic plane (Aharonian et al. 2005b, 2006k) performed with the H.E.S.S. telescopes has revealed a comparably small number of shell-type SNR while VHE emission from pulsar wind nebula (PWN) systems has been observed more frequently (Gaensler & Slane 2006). In total, 20 VHE sources (including candidate associations) have been discovered which are very likely powered by isolated pulsars.

The population of “TeV-Plerions” (Horns et al. 2006) includes young objects like Kes-75/PSR J1846-0258 (spin-down age  $\tau = 723$  yrs) (A. Djannati-Atai et al. 2007), MSH 15-52 (Aharonian et al. 2005c) driven by PSR J1513-5908 ( $\tau = 1.55$  kyrs) as well as evolved systems like the PWN driven by PSR B1823-13 ( $\tau = 21.4$  kyrs) associated with HESS J1825-137 (Aharonian et al. 2005j). Apparently, PWN systems are active VHE sources for a few 10 000 years thus exceeding the time that a SNR evolves through the Sedov-stage of shell type SNR during which presumably VHE emission is most likely produced. The longer time during which PWNs are active particle accelerators explains the larger number of PWN systems active at any given time in the Galaxy in comparison to shell-type SNRs.

However, the contribution of PWN to the Galactic cosmic rays remains an open question as long as the nature of the particles accelerated in these systems is not clarified. Currently, for most of the VHE emitting PWNs, a leptonic origin of the VHE emission can qualitatively explain the multiwavelength morphology and energy spectra. As an example, HESS J1825-137 has been studied intensively both in X-rays as well as in VHE-gamma-rays where the source extension appears to be larger by a factor of  $\approx 6$  than in the X-ray band. This larger size can be explained by a greater loss time of electrons radiating VHE gamma-rays via inverse Compton scattering than the loss time of electrons radiating synchrotron X-rays (Aharonian et al. 2006h). The energetic electrons injected by the pulsar PSR B1823-13 lose rapidly energy in the high magnetic field environment close to the pulsar where the X-ray nebula is observed (Gaensler et al. 2003). While the particles leave the high magnetic field environment, they presumably radiate only at wave-lengths longer than the X-ray band in the synchrotron channel while inverse Compton scattering off the cosmic microwave-background is the dominant energy loss process leading to observable, extended VHE emission. In this model, the slowly decaying spin-down power of the pulsar is accumulated in an expanding bubble containing the TeV-emitting electrons. This scenario is supported by softening of the observed VHE spectra with increasing distance to the compact X-ray PWN system (Aharonian et al. 2006h).

The observed morphology of the PWN is often asymmetric and not centered on the pulsar. While in some cases, the velocity of the pulsar can accommodate for the offset, other objects require an alternative explanation (e.g. Vela X): here, the asymmetric reverse shock of the SNR shell interacts with the relativistic PWN gas “crushing” and pushing it off-centered (Blondin et al. 2001; Ferreira & de Jager 2008).

A contribution to the observed VHE gamma-ray flux from nuclei accelerated by the pulsar is not excluded but seems to be less important than the contribution of electrons for most systems.

The Vela-X PWN system may be an exception. Here, the spin down power of the pulsar is by far larger than the acceleration rate of electrons required to drive the PWN system. In this sense, there is missing energy that can be naturally explained by a nucleonic component in the wind that drives the acceleration of electrons through resonant wave absorption (Arons & Tavani 1994) and produces the bulk of the observed VHE emission (Aharonian et al. 2006i). The VHE spectrum can be explained quite well in terms of over-all energetics (thus solving the problem of "missing" energy) as well as its shape (Horns et al. 2006). A crucial test will be the detection of high energy neutrinos from this object that may be the brightest steady neutrino source in the sky (Kappes et al. 2007b,a).

Finally, composite systems where a plerionic, non-thermal X-ray component is observed to be embedded in a radio-emitting shell like G0.9+0.1 have been found to emit VHE gamma-rays (Aharonian et al. 2005g). In addition to known composite SNRs, VHE observations have helped to discover and identify new systems: X-ray observations of HESS J1813-178 (Aharonian et al. 2005b) carried out with XMM-Newton have revealed a previously unknown extended X-ray source inside the radio-shell of SNR G12.82-0.02 (Funk et al. 2007) putting this object in the category of composite SNR systems. Most likely, the VHE-emission is produced in the central PWN systems while the radio-shell is VHE-dim. However, it should be noted, that the spatial extension of these two systems is barely resolved at VHE energies.

### 3.4 X-ray binary systems

Before the imaging air Cherenkov technique was widely established, several groups had claimed a number of X-ray binary sources to be periodic (e.g Her X-1, Cyg X-3). Cyg X-3 had been claimed to be a transient source of energetic particles up to PeV energies (Samorski & Stamm 1983), for a review of early claims of detections see Weekes (1992). With the notable exception of a possible burst observed from the direction of GRS 1915+105 (Aharonian & Heinzlmann 1998), none of the XRB systems had been confirmed until recently to be VHE gamma-ray emitters. Finally 4 XRB systems listed in Table 2 have been detected to be VHE gamma-ray sources. All of these objects show variability in the VHE band either linked to the orbital motion as for LS I +61 303 (Albert et al. 2006f; Maier 2007), LS 5039 (Aharonian et al. 2006c), and PSR B1259-63 (Aharonian et al. 2005d), or transient activity as for Cyg X-1 (Albert et al. 2007h).

Given that these objects are currently the only variable Galactic sources of VHE gamma-rays, the interpretation of their properties is quite different from the other source types. The orbital parameters as well as the physical conditions in these systems are reasonably well-known and allow for a detailed modelling of the processes leading to acceleration and VHE emission. In this sense, one can consider the systems as "laboratories".

The pulsar PSR B1259-63 ( $P = 48$  ms) is in a highly eccentric orbit ( $P_{\text{orbit}} = 3.4$  yrs) around the Be-type companion star SS2883. VHE emission is predomi-

Table 2: X-ray binary systems detected with imaging air Cherenkov telescopes..

Identifier	Variability	D [kpc]	$L^a$ [ $10^{33}$ ergs/s]	System <sup>b</sup>
PSR B1259-63	$P = 3.4$ a	1.5	1.6	PSR(47 ms)/B2e
LS 5039	$P = 3.9$ d	2.5	8.7	BH or NS/O6.5V
LS I +61 303	$P = 26.5$ d	2	2.5	NS/B0Ve
Cyg X-1	$T_{\text{var}} \approx 80$ min	2.2	1.6	BH/O9.7 Iab

<sup>a</sup>Integrated from 1 to 10 TeV

<sup>b</sup>BH: Black hole candidate, NS: Neutron star, PSR: Pulsar

nantly produced around the periastron where the effects of adiabatic and radiative cooling due to inverse Compton as well as synchrotron emission are strongest (Aharonian et al. 2005d). The IC component had been predicted successfully prior to the detection (Kirk et al. 1999), albeit the observed temporal behavior of the source as it passed through the periastron in 2004 was quite different from the expectation (Aharonian et al. 2005d). Refined models including a more detailed treatment of inverse Compton scattering in energetic and anisotropic radiation fields as well as adiabatic energy losses can reproduce the observed light curve and provide some crucial predictions to be probed with new observations (Khangulyan et al. 2007). Alternative models invoking the presence of a nucleonic component that leads to VHE emission through the interaction with the disk-outflow of the Be-star have been proposed as well (Kawachi et al. 2004; Neronov & Chernyakova 2007).

Unfortunately, the periastron passage in 2007 took place during the time when PSR B1259+63 culminated during the day time. A crucial observation will be only possible during the periastron passage in 2011 when the system will be visible for ground based VHE instruments as well as for Fermi.

The two systems LS 5039 as well as LS I +61 303 have shorter orbital periods of 3.9 and 26.5 days, respectively. Initially, both objects have been considered to be micro-quasars with a steady radio-jet feature. There is an ongoing debate whether this picture may have to be modified. Radio observations of LS I+61 303 indicate that the orientation of the "jet" changes during the orbit (Dhawan et al. 2006) which is more in line with the cometary tail predicted by Dubus (2006b). The cometary tail is a consequence of the interaction of a pulsar wind with the stellar outflow. For LS 5039, the current high resolution radio observations also indicate a change in the orientation of the jet-like structure (Ribó et al. 2008). However, since the observations do not cover a full orbital period, the results are not conclusive yet.

Given the uncertainty of the nature of the compact object, the VHE emission from LS 5039 has been interpreted in the context of a micro-quasar model (Bosch-Ramon et al. 2006) as well as in an interacting PWN model (Dubus 2006b).

A crucial consideration is the absorption of VHE photons due to pair-production in the photon field of the stellar companion. If the line-of-sight towards the VHE emission region passes within roughly  $10^{14}$  cm of the companion star of LS 5039, absorption will produce visible effects (Dubus 2006a) varying with the phase of the orbit. The absorption effect is energy dependent and should lead to a pronounced



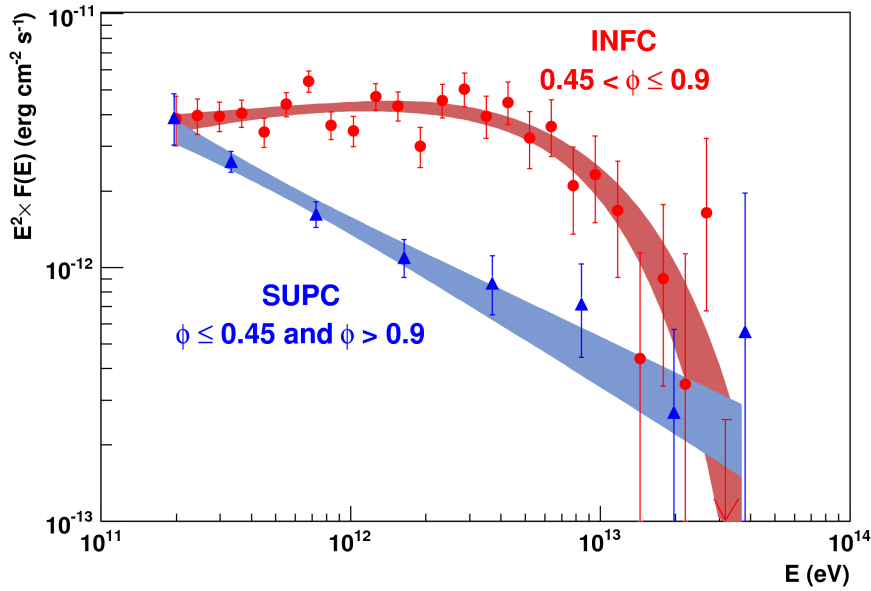


Figure 4: The VHE energy spectrum of LS 5039 for two distinct orbital phases. The *INFC* corresponds to the inferior conjunction, while *SUPC* is the phase interval at the superior conjunction with the periastron passage (Aharonian et al. 2006c).

variability at energies between 200-400 GeV. However, the observations indicate that the flux at 200-400 GeV remains almost unchanged along the orbit while the modulation is most pronounced at TeV-energies (see Fig. 4).

Secondary particle production in cascades can in principle reproduce the observed variability (Bednarek 2007b) as well as models where the emission takes place at a larger distance to the stellar companion (Khangulyan et al. 2008).

### 3.5 Star-forming regions

So far, the objects under scrutiny are related to the final stages of stellar evolution and their remnants. However, gamma-rays are also produced in molecular clouds which are the cradles of star formation and possibly during the final mega-year of stellar evolution where massive stars ( $> 15 M_{\odot}$ ) drive powerful winds. The wind-phase of stellar evolution is characterized by mass loss rates of up to  $10^{-5} M_{\odot}/\text{year}$  and terminal velocities of a few 1000 km/s. These early-type stars are usually born in open stellar associations in the spiral arms of the Galactic disk. The massive O stars in these associations often evolve into the Wolf-Rayet phase where strong stellar winds produce a hot tenuous cavity in the interstellar medium. In such systems up to  $10^{39}$  ergs/s are dissipated in the form of kinetic energy from stellar winds, even before member stars evolve into supernovae. Provided that shocks will form either in the termination region of cumulative winds (Domingo-Santamaría & Torres 2006)

or in wind-wind interaction regions (Reimer et al. 2006; De Becker 2007), some of this power can be converted into cosmic-ray acceleration.

The detection of VHE-emission from Westerlund-2 is a crucial step towards establishing the rôle of stellar driven cosmic ray acceleration (see Fig. 5 from Aharonian et al. (2007d)). Westerlund-2 is a young star forming region with roughly 20 O-type stars and the Wolf-Rayet systems WR 20a&b (Rauw et al. 2007). The total power released in the stellar winds is estimated to be  $5 \times 10^{37}$  ergs/s. The observed VHE emission can be easily produced if roughly 1 % of the kinetic energy is converted into the acceleration of electrons (Manolakou et al. 2007; Reimer et al. 2007).

Prior to the discovery of VHE emission from Westerlund-2, the first unidentified VHE source TeV J2032+4130 had been associated with the remarkably powerful OB association in the Cygnus arm. The HEGRA discovery of TeV J2032+4130 (Aharonian et al. 2002a, 2005a) has been recently confirmed by MAGIC (Albert & for the MAGIC Collaboration 2008) as well as by the MILAGRO and VERITAS groups (Abdo et al. 2007a,b; Lang et al. 2004; Konopelko et al. 2007). Remarkably, observations with the MILAGRO detector show an extended ( $\approx 3^\circ$ ) source of  $> 10$  TeV photons centered on TeV J2032+4130 (Abdo et al. 2007a). This source has received considerable multi-wavelength coverage including deep radio observations which show indications for extended radio emission coinciding with the VHE source (Paredes et al. 2007). Recent X-ray observations with XMM-Newton have revealed faint non-thermal extended X-ray emission co-located with the VHE-source (Horns et al. 2007).

Future observations of this region with the VERITAS telescope array will be very helpful to disentangle possible multiple-sources and to study the source size at different energies.

Besides Westerlund-2 and Cyg OB2, the MILAGRO source MGRO J2019+37 (Abdo et al. 2007a) has been associated with the young stellar association Berk-87 including the Wolf-Rayet object WR 142 (Bednarek 2007a).

A systematic search for VHE emission with the HEGRA telescopes from young open clusters has so far produced only upper limits (Aharonian et al. 2006a).

### 3.6 Unidentified Galactic sources

The sources discussed in the previous section have been identified or are associated with known objects. However, a number of objects remain to be identified. A total of 10–20 objects have no clear or even multiple counterparts. Among these objects, the Galactic center source and the point-like source in the Monoceros region are highlighted in the following. For a recent summary of unidentified sources, see e.g. Funk (2007); Aharonian et al. (2008c).

**Galactic center region.** The central region of our Galaxy contains a super-massive black hole with a mass of  $3 \times 10^6 M_\odot$  (Schödel et al. 2002; Ghez et al. 2005). Given the faintness of this object, the accretion rate must be  $< 10^{-8}$  of the Eddington-rate. The mm-, IR-, and X-ray sources associated with Sgr A\* have been observed to show variability including flares and outbursts with a time-scale of hours (Genzel et al. 2003). The shortness of the flares constrains the emission region to be compact with

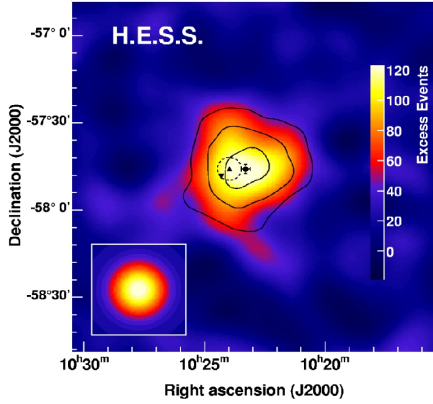


Figure 5: Westerlund 2 (Aharonian et al. 2007d): The color scale indicates the smoothed VHE excess map (see the bottom left inlaid figure for the point-spread function), the contours are the significance levels starting at  $5\sigma$  and increasing by 2. The filled circle and error bars mark the position and uncertainty of the VHE source ( $1\sigma$ ). The dashed circle marks the position and extension of Westerlund 2, the upright triangle is at the position of the Wolf-Rayet binary system WR 20a and the downward triangle is at the position of WR 20.

a spatial extension  $r < t_{var} \cdot c \approx 10^{14}$  cm ( $t_{var}/hr \approx 100r_G(M/3 \cdot 10^6 M_\odot)^{-1} t_{var}/hr$ ). Observations with the CANGAROO III telescopes as well as at large zenith angles with the Whipple 10m telescope revealed a VHE gamma-ray source co-located with the Galactic center (Tsuchiya et al. 2004; Kosack et al. 2004). The positional accuracy as well as spectral measurements have been considerably improved with the observations of the H.E.S.S.-telescopes (Aharonian et al. 2004b). The MAGIC telescope has confirmed the earlier findings in independent observations (Albert et al. 2006d).

The detection of a point-like source with a hard power-law spectrum was shortly after the discovery discussed in the context of emission scenarios near to the supermassive black hole (at distances larger than  $\approx 10 r_G$  in order to avoid internal absorption) from e.g. ultra-high energy protons emitting synchrotron and curvature radiation in the high magnetic fields that are believed to be threaded in the accretion disk (Aharonian & Neronov 2005) or  $\pi^0$ -decay from energetic protons (Ballantyne et al. 2007; Liu et al. 2006). At a larger distance from Sgr A\*, acceleration in SNRs (Erlykin & Wolfendale 2007) including Sgr A East (Crocker et al. 2005) as well as acceleration in stellar winds have been proposed (Quataert & Loeb 2005).

The initial data were consistent with a Dark Matter annihilation scenario albeit requiring uncomfortably large masses beyond 20 TeV for the annihilating particles (Horns 2005).

With more data, the H.E.S.S. experiment has constrained the energy spectrum to extend beyond 10 TeV and to deviate from a WIMP-annihilation scenario (Aharonian et al. 2006j)<sup>14</sup>. With the increased exposure, faint spatially extended VHE emission along the Galactic ridge was detected (Aharonian et al. 2006g). The accuracy of reconstruction the position of the VHE-emitting point source has been improved to the

<sup>14</sup>see however Bringmann et al. (2008) for a discussion on the effects of internal Bremsstrahlung photons which are important for heavy WIMP annihilation in order to reduce the helicity suppression for the annihilation channel

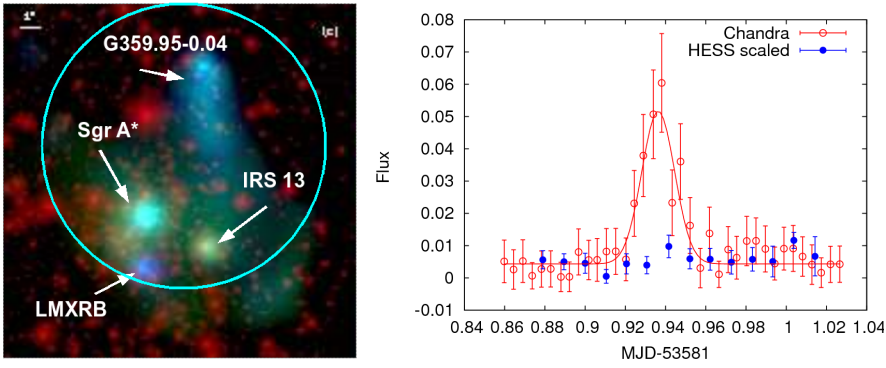


Figure 6: **Left panel:** Chandra X-ray and SINFONI near-IR composite from Wang et al. (2006) with additional annotations. The circular region corresponds to the combined systematic and statistical uncertainty for the HESS-source associated with the Galactic center. **Right panel:** X-ray and VHE-gamma-ray light curve from simultaneous observations of Sgr A\*. The H.E.S.S. light curve has been scaled to match the Chandra light curve in units of counts per second. Note the comparably small error bars of the H.E.S.S. observations - a flare of similar magnitude as observed in the X-ray band would have been clearly detected.

level of the systematic pointing uncertainty of  $\approx 6$  arc seconds (van Eldik et al. 2007) and excludes Sgr A East. The error box for the VHE source still encompasses at least three possible candidates for VHE emission (see Fig. 6a): Sgr A\*, a low-mass X-ray binary system (LMXRB) (Muno et al. 2005), the stellar system IRS 13 (Baganoff et al. 2003), and the PWN G359.95-0.04 (Wang et al. 2006). The PWN system has been argued to be a possible candidate to explain the observed VHE emission (Hinton & Aharonian 2007).

An association with a variable source like Sgr A\* would be supported if simultaneous multi-wavelength (MWL) observations of Sgr A\* during an outburst would show a correlation between e.g. X-ray and gamma-ray flux. During a dedicated MWL observation of Sgr A\* in summer 2005 with H.E.S.S. and the Chandra X-ray telescope, a typical X-ray flare was detected with the Chandra instrument (Hinton et al. 2007a). The simultaneously taken H.E.S.S.-data show however no variability even though the observed rate of VHE photons is sufficiently large to detect a flare of similar strength as seen in the Chandra data (see Fig. 6b). The absence of correlation would disfavor at least a common origin of the X-ray and VHE emission from Sgr A\*.

An association of the VHE source with the LMXRB could in principle be demonstrated by correlated activity in different wavelength-bands. However, so far no such observations are available.

At this point it is not possible to discern between the different source candidates nor exclude a dark matter origin.

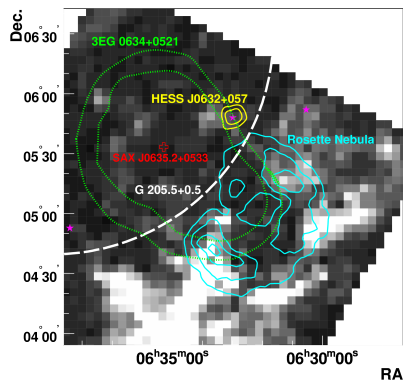


Figure 7: Monoceros source (Aharonian et al. 2007h): The grey-scale illustrates the velocity-integrated ( $0\text{-}30 \text{ km s}^{-1}$ )  $^{12}\text{CO}$  emission as measured with the NANTEN telescope (Mizuno & Fukui 2004). The yellow-contours trace the 4 and 6  $\sigma$  level of detection with the H.E.S.S. telescopes. The cyan contours indicate the 8.35 GHz radio measurements from Langston et al. (2000) while the green contours mark the 95 % and 99 % confidence regions for the position of the EGRET source 3EG 0634+0521. SAX J0635.2+0533 is a pulsar binary system. The positions of Be-stars are indicated with pink stars.

**Monoceros source.** The newly discovered population of unidentified VHE sources in the Galactic plane form a quite homogeneous sample of objects with respect to their spatial extension and energy spectra. It should be emphasized however, that the similarity of the VHE characteristics does not necessarily imply that the underlying sources are similar. Certainly, observational biases are introduced by e.g. the limited sensitivity for detecting sources with low surface brightness.

Among the unidentified sources, there is - besides the Galactic center - only one more unresolved object: HESS J0632+058 which is close to the rim of the Monoceros Loop SNR (Aharonian et al. 2007h). The radial extension of this object is constrained to be smaller than  $2'$  (95% c.l.). No strong indications for variability are observed. The energy spectrum of the source is well-described by a power-law ( $dN/dE \propto E^{-2.5 \pm 0.3}$ ) which is at the soft end of the distribution of energy spectra observed from unidentified VHE-sources.

For an unresolved source ( $r < 2'$ ), the search for a counterpart is simpler than for extended objects. In Fig. 7, the position of HESS J0632+058 is combined with multi-wavelength observations. Only a few candidate objects coincide spatially with the VHE source including an unidentified EGRET source 3EG J0634+0521 (Hartman et al. 1999), an unidentified X-ray source 1RXS J063258.3+054857 (Voges et al. 2000), and a B0pe type star MWC 148 which may be a binary system similar to PSR B1259-63. Alternatively, it could be a new type of VHE source associated with an isolated stellar system.

### 3.7 Extra-galactic sources

The blind survey of the Galactic plane has revealed an interesting and previously unknown population of VHE-sources. Unfortunately, a survey with similar sensitivity of the extra-galactic sky has to be postponed until wide-field-of-view Cherenkov telescopes or the next generation of Water-Cherenkov-experiments like HAWC will

come online (see also next section). Currently, the observations have focussed on Blazars ("BL Lac type Quasars").

Historically, the discovery of VHE emission from the Blazars Mkn 421 (Punch et al. 1992) and Mkn 501 (Quinn et al. 1996) have opened the field of TeV-Blazar observations. These objects are in general characterized by a featureless optical spectrum, non-thermal X-ray emission, and violent variability in the optical wavelength-band as well as in X-rays. The spectral energy distribution is dominated by two broad maxima - one in the optical-to-X-rays and one in the gamma-ray-to-VHE-gamma-ray domain. The low-energy maximum is usually assumed to be produced by synchrotron emitting electrons while the high energy bump would be due to inverse-Compton scattering.

TeV-Blazars can be considered "clean" systems where the main source of seed photons are actually the synchrotron photons emitted by the electrons themselves, commonly called Synchrotron-Self-Compton (SSC) mechanism. Within the unified scheme, Blazars are believed to be Fanaroff-Riley Type I galaxies with a jet axis pointing close to the line-of-sight.

In a simple one-zone-SSC model, the VHE luminosity is closely linked to the synchrotron luminosity which in turn is related to the particle density and provides seed photons for inverse Compton scattering. A simple but very successful selection scheme of possible VHE emitting candidates is based on the X-ray or radio flux of Blazars (Costamante & Ghisellini 2002). Most of the Blazars that have been predicted to be detectable according to this scheme have been actually discovered by the H.E.S.S. and MAGIC collaboration.

With the growing number of known Blazars at different red-shifts (see Table 3 for a list of extra-galactic VHE-gamma-ray sources), a number of issues and questions can be addressed:

- Is a simple one-zone SSC model sufficient to explain all (multi-wavelength) data including correlated variability patterns or is a more complicated model required (stratified jets, multiple zones model)?
- Where does the acceleration take place?
- What is the underlying acceleration mechanism in Blazars and what is the composition of the jet? This is a fundamental question related to the jet physics and the energetics of AGN.
- What is the duty cycle of Blazars?
- How strong is the beaming? In the relativistic outflow, a co-moving isotropic emission is strongly beamed in the forward direction. With increasing bulk Lorentz factor  $\Gamma$ , the opening angle gets narrower  $\propto \Gamma^{-1}$ . The higher the beaming, the smaller the likelihood that we can observe the emission. In consequence, a high beaming factor can lead to dramatically increased number of Blazars that are pointing *not* in our direction.
- Is there internal absorption (due to photon-photon scattering with pair-production)?
- How strong is the absorption on the extra-galactic background light (EBL)?

In the following, I will highlight observations from Blazars as well as from non-Blazar VHE sources including M87 and the flat-spectrum-radio quasar 3C279.

### 3.8 Blazars

A very spectacular feature of VHE emission from Blazars is the short time-scale variability. The most impressive examples of short flares have been observed in 2006 from the nearby object PKS 2155-305 (red-shift  $z = 0.116$ ). This object was the first Blazar discovered in the southern hemisphere by the Durham group using their Mark VI telescope in Australia (Chadwick et al. 1999). The H.E.S.S. telescopes observed their “first gamma-light” from this source already in 2002 when the first of the four H.E.S.S. telescopes went online (Punch 2007). Since PKS 2155-305 is a remarkably bright object, it can be easily detected in quiescent state with the system of four H.E.S.S. telescopes. Detailed measurements of the energy spectrum show despite widely different flux states only marginal deviations from a soft power-law with photon index  $\approx 3.3$  (Aharonian et al. 2005f). PKS 2155-305 has been the target of a number of simultaneous multi-wavelength-campaigns together with the RXTE X-ray satellite as well as in conjunction with the Chandra, XMM-Newton, and the SWIFT X-ray telescopes (Aharonian et al. 2005i). During summer 2006, the source went into an unprecedented high state reaching flux levels more than a factor of 100 higher than the quiescent flux (Aharonian et al. 2007c). During the peak flares, the rate of detected VHE gamma-rays reached values exceeding 1 Hz which marks the highest rate ever detected at VHE energies. During the night with the highest flux, a sequence of flares can be discerned with rise and decay timescales of minutes (see Fig. 8). This immediately constrains the emission region to be very compact and to be moving with a large bulk Lorentz factor to overcome pair-opacity and to relax the size constraint (Begelman et al. 2008). Under the assumption that the variable emission is produced close to the super-massive black hole, two interesting conclusions have been pointed out recently: (a) The variability time scale constrains the mass of the black hole to be of the order of  $10^7 M_{\odot}$  roughly 2 orders of magnitude smaller than the general correlation of the mass with luminosity of the host galaxy suggests (Celotti et al. 1998; Neronov et al. 2008; Bettoni et al. 2003). (b) The apparent periodicity of the subflares observed could potentially provide a measure of the angular momentum of the black hole (Neronov et al. 2008).

### 3.9 Other active galactic nuclei

Besides the Blazars, only two non-Blazar extra-galactic objects have been discovered so far: M 87 and 3C 279<sup>15</sup>

**M87** Besides the collective study of a Blazar sample (Wagner 2008), it is interesting to closely examine nearby FR-I radio galaxies as these objects are considered to

---

<sup>15</sup>A signal from Centaurus A at energies above 300 GeV had been claimed on the basis of non-imaging observations of air Cherenkov light at the level of  $4.5 \sigma$  (Grindlay et al. 1975). This claim awaits confirmation.

Table 3: List of extragalactic VHE-sources sorted by red-shift. Whenever available, different source activity states are characterized .

Source	Type	$z$	$d_L^a$	$\log_{10}(L_\gamma)^b$	$\Gamma_{\text{measured}}$	Ref.
M87	FR I	0.0044	23	41.1	$2.6 \pm 0.4$	<sup>c</sup>
				41.6	$2.2 \pm 0.2$	<sup>c</sup>
Mkn 421	HBL	0.030	130	44.8	$3.0 \pm 0.2$	<sup>d</sup>
				45.3	$2.06 \pm 0.03$	<sup>d</sup>
Mkn 501	HBL	0.034	142	44.3	$2.45 \pm 0.07$	<sup>e</sup>
				45.2	$2.09 \pm 0.03$	<sup>e</sup>
1ES 2344+514	HBL	0.044	183	43.9	$2.9 \pm 0.2$	<sup>f</sup>
				45.2	$2.5 \pm 0.2$	<sup>g</sup>
Mkn 180	HBL	0.045	194	44.0	$3.3 \pm 0.7$	<sup>h</sup>
1ES 1959+650	HBL	0.047	198	44.2	$2.7 \pm 0.1$	<sup>i</sup>
				44.9	$1.8 \pm 0.2$	<sup>j</sup>
BL Lacertæ	LBL	0.069	293	44.0	$3.6 \pm 0.5$	<sup>k</sup>
PKS 0548-322	HBL	0.069	300	43.6	$2.8 \pm 0.3$	<sup>l</sup>
PKS 2005-489	HBL	0.071	306	44.2	$4.0 \pm 0.4$	<sup>m</sup>
RGB J0152+017	HBL	0.080	345	44.0	$3.0 \pm 0.4$	<sup>n</sup>
W Comae	IBL	0.102	452	44.9	$3.8 \pm 0.4$	<sup>N</sup>
PKS 2155-304	HBL	0.116	515	44.1	$3.4 \pm 0.1$	<sup>o</sup>
				46.8	$2.7 \pm 0.1$	<sup>p</sup>
			Break at 0.43 TeV		$3.5 \pm 0.1$	<sup>p</sup>
H 1426+428	HBL	0.129	585	45.9	$3.7 \pm 0.4$	<sup>q</sup>
1ES 0806+524	HBL	0.138	626	43.8	assumed 2.6	<sup>Q</sup>
1ES 0229+200	HBL	0.139	633	44.3	$2.5 \pm 0.2$	<sup>r</sup>
H 2356-309	HBL	0.165	758	44.5	$3.1 \pm 0.2$	<sup>s</sup>
1ES 1218+304	HBL	0.182	855	45.2	$3.0 \pm 0.4$	<sup>t</sup>
1ES 0347-121	HBL	0.185	864	44.8	$3.1 \pm 0.3$	<sup>u</sup>
1ES 1101-232	HBL	0.186	877	44.8	$2.9 \pm 0.2$	<sup>v</sup>
1ES 1011+496	HBL	0.212	1008	45.5	$4.0 \pm 0.5$	<sup>w</sup>
PG 1553+113	HBL	> 0.3	> 1498	> 46.1	$4.5 \pm 0.3$	<sup>x</sup>
		< 0.74	< 4437	< 47.1		<sup>x</sup>
S5 0716+714	IBL	0.31	1557	46.1	assumed 3.8	<sup>XY</sup>
3C279	FSRQ	0.536	2998	46.7	$4.1 \pm 0.7$	<sup>y</sup>

<sup>a</sup>Assuming  $\Omega_m = 0.27$ ,  $\Omega_\Lambda = 0.73$ ,  $H_0 = 73 \text{ km s}^{-1} \text{ Mpc}^{-1}$

<sup>b</sup>Isotropic luminosity  $L_\gamma$  in  $\text{ergs s}^{-1}$  integrated between 0.1 and 1 TeV

<sup>c</sup>Aharonian et al. (2006b), <sup>d</sup>Aharonian et al. (2002b), <sup>e</sup>Albert et al. (2007g), <sup>f</sup>Albert et al. (2007e), <sup>g</sup>Schroedter et al. (2005), <sup>h</sup>Albert et al. (2006b), <sup>i</sup>Albert et al. (2006e), <sup>j</sup>Aharonian et al. (2003a), <sup>k</sup>Albert et al. (2007d), <sup>l</sup>The H. E. S. S. Collaboration (2007), <sup>m</sup>Aharonian et al. (2005e), <sup>n</sup>HESS Collaboration: F. Aharonian (2008), <sup>N</sup>Acciari et al. (2008a), <sup>o</sup>Aharonian et al. (2005f), <sup>p</sup>Aharonian et al. (2007c), <sup>q</sup>Djannati-Ataï et al. (2002), <sup>Q</sup>Swordy (2008), <sup>r</sup>Aharonian et al. (2007b), <sup>s</sup>Aharonian et al. (2006f), <sup>t</sup>Albert et al. (2006a), <sup>u</sup>Aharonian et al. (2007a), <sup>v</sup>Aharonian et al. (2007e), <sup>w</sup>Albert et al. (2007a), <sup>x</sup>Aharonian et al. (2008a), <sup>X</sup>Nilsson et al. (2008), <sup>Y</sup>Teshima & The MAGIC Collaboration (2008), <sup>y</sup>Albert et al. (2008)



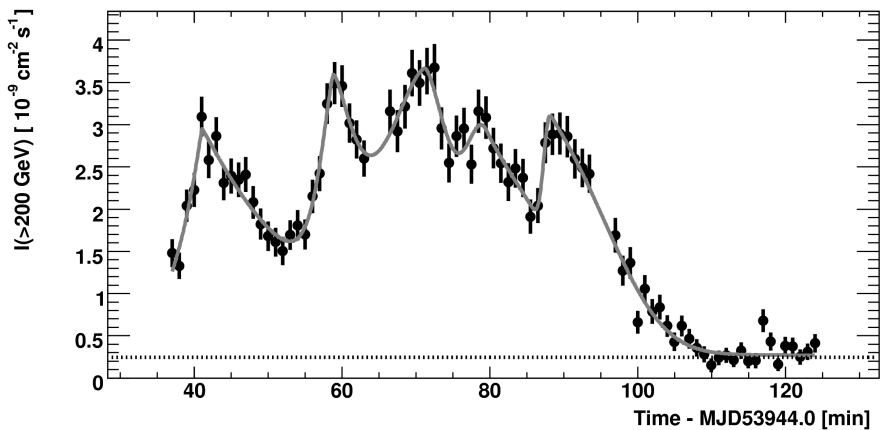


Figure 8: The light curve from PKS 2155-304 in the night July-28 2006 as measured with H.E.S.S. above 200 GeV. The data are binned in 1-minute intervals. For comparison, the horizontal dotted line represents  $I(>200 \text{ GeV})$  observed from the Crab Nebula. The curve is a fit of a superposition of five individual bursts and a constant flux. See Aharonian et al. (2007c) for additional details.

be mis-aligned Blazars. The closest FR-I objects are M87 and Cen-A. VHE gamma-ray emission from M87 had been initially reported from the HEGRA group (Aharonian et al. 2003b) and later verified by the Whipple collaboration (Le Bohec et al. 2004), as well as by the H.E.S.S. group (Aharonian et al. 2006b) and most recently with the VERITAS telescopes (Acciari et al. 2008b).

While the initial sensitivity was only sufficient to detect a signal and coarsely constrain the energy spectrum, following observations mainly with the H.E.S.S. telescopes have lead to a number of important discoveries: the energy spectrum of M87 extends to energies beyond 10 TeV and even more spectacular, the observed emission is highly variable on time-scales as short as days (Aharonian et al. 2006b). The hard spectrum is a surprise and disfavors the models suggested by Georganopoulos et al. (2005) and Reimer et al. (2004) where the predicted gamma-ray spectrum is soft as a consequence of the assumption of a small Doppler-factor derived from radio measurements of the jet dynamics. It should be noted however, that also other nearby Blazars that have been observed with high resolution radio interferometers do not show strong super-luminal motion indicative for large Doppler-factors. It seems that there is growing evidence for a discrepancy between high Doppler factors implied by modelling the VHE emission of Blazars with single zone SSC model and the lack of evidence for strong super-luminal motion in these objects from radio observations (Piner et al. 2008). The fast variability observed from M87 leads to interesting implications. First of all, the variability excludes models where the VHE gamma-rays are produced in processes like Cosmic ray interactions in the host galaxy (Pfrommer & Enßlin 2003) or even Dark Matter annihilation (Baltz et al. 2000). These processes should not lead to temporal variation of the observed emission. Given that the vari-

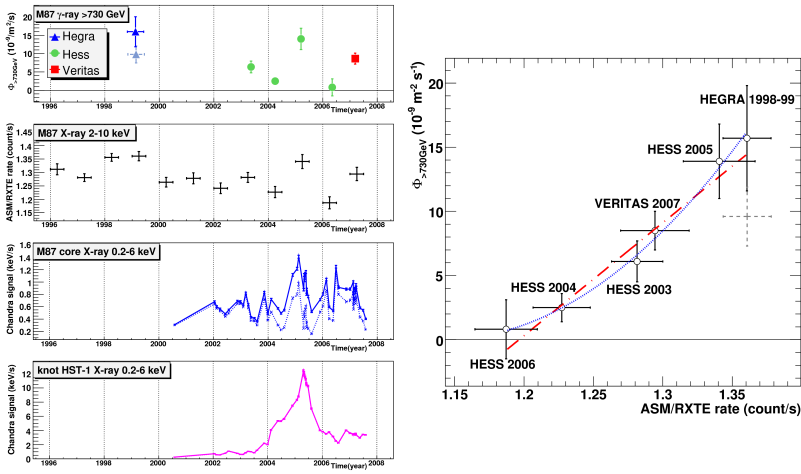


Figure 9: From Acciari et al. (2008b): The left panel combines the VHE and X-ray light curves from observations of M87 with ground based Cherenkov telescopes as well as with satellite instruments on-board the RXTE satellite (ASM) and the Chandra observatory. The right panel correlates the yearly VHE fluxes with the appropriately averaged ASM fluxes. The dashed curve is a linear correlation and the solid curve a squared function.

ability time scale can not be smaller than the light crossing time, the constraint on the size of the emission region is severe and excludes regions in the outer radio jet as well. A possible candidate for the emission could be the notoriously variable HST-1 knot located less than 1 arc sec off the core. The most recent long-term light-curve obtained with the all-sky-monitor on-board the RXTE satellite as well as a dedicated Chandra monitoring seems to support a correlation of the HST-1 activity in X-rays and the observed VHE emission (see Fig. 9).

**3C279** This object belongs to the so-called flat-spectrum radio quasars (FSRQs). These objects are long-known to be emitters of GeV gamma-rays that have been detected with EGRET (Hartman et al. 1992, 2001). There are two aspects which single out this source: (a) 3C279 has a comparably large red-shift of  $z = 0.536$  and (b) it is a new type of AGN which shows acceleration to TeV energies.

The EGRET Blazars are mostly members of the FSRQ-class and are characterized by a spectral energy distribution with a peak in the EGRET energy range, dominating the total luminosity. The observed emission is commonly attributed to external Comptonization of photons from the broad-line region and possibly from the accretion disk. Given that FSRQs have intrinsically a higher gamma-ray luminosity than Blazars, they can be in principle observed to higher red-shifts opening up the possibility to finally detect absorption features in the VHE gamma-ray spectra (see also next section) of extra-galactic objects (see also next section). The detection of VHE emission from 3C279 with the MAGIC telescope (Teshima et al. 2007) indicates

variability which seems to be correlated with changes in the optical flux. Further observations of this source and a measurement of the VHE energy spectrum could provide important clues on the level of extra-galactic background light (see next section). Even in the case of a low level of EBL, only  $10^{-3}$  of the emitted flux will be observable at 1 TeV (Raue & Mazin 2008).

## 4 "Secondary physics": Propagation of gamma-rays

### 4.1 EBL absorption

VHE emission from AGN appears to be more common than what could have been hoped for and the temporal variability observed at the highest energy is providing us an important and unique in-sight into the “engine-room” of AGN. The understanding of processes leading to VHE-emission hinges however on a good understanding of pair-absorption processes of the type  $\gamma_{\text{VHE}}\gamma_{\text{EBL}} \rightarrow e^+e^-$ . This process has been known for a long time to be relevant for the propagation of TeV-photons over cosmological distances (Gould & Schröder 1966).

With the growing number of Blazars observed at various red-shifts it has become feasible to use VHE-photons as *probes* to constrain or even measure the background photon density in extra-galactic space. Until now, it has however not been possible to clearly establish absorption in the measured Blazar spectra because the intrinsic emission spectrum is not very well known and may suffer additional internal absorption (Aharonian et al. 2008d). When invoking a constraint on the shape of the intrinsic spectrum, it is however possible to derive (model-dependent) upper limits on the EBL density (Dwek & Krennrich 2005; Aharonian et al. 2006e; Mazin & Raue 2007). The situation will be greatly improved when the first broad-band spectra of Blazars will be obtained that should show a transition from the optically thin to the optically thick part. The detection of such an absorption feature will in turn lead to a detection of the EBL. In combination with increasing statistics and coverage over varying red-shift, it will be feasible to investigate the evolution of the EBL and finally, derive in a completely independent way constraints for cosmological parameters (Blanch & Martinez 2005a,b).

### 4.2 Lorentz invariance violation

VHE photons are useful probes for Lorentz invariance violating (LIV) processes. A number of theoretical approaches towards a quantum theory of Gravity predict a structure of space-time at the Planck scale. This will result in a modified dispersion relation for photons of the form  $c^2p^2 = E^2(1 + \xi(E/M_{\text{QG}}) + \mathcal{O}(E/M_{\text{QG}})^2)$  see e.g. Sarkar (2002) for a review. This dispersion relation affects the time-of-flight of photons of different energies and the kinematics of interaction, suppressing e.g. the pair-production process of photons.

Currently, fast flares from Mkn 421 (Gaidos et al. 1996), Mkn 501 (Albert et al. 2007g), and PKS 2155-304 (Aharonian et al. 2007c) have been observed. The latter is potentially the most constraining observation as the red-shift is larger and the vari-

ability faster as well as more photons have been collected than for the other sources. Current limits on  $M_{\text{QG}} > 3 \times 10^{17}$  GeV (Albert et al. 2007i) are already an order of magnitude better than limits obtained from GRBs (Ellis et al. 2003, 2006). It is important to point out that if a dispersion of arrival times from flares is detected, source intrinsic spectral variations can be excluded once consistent time lags are detected from a sample of flares from different sources at different red-shifts. Ultimately, the inferred LIV characteristics should be consistent with a suppression of EBL absorption processes.

## 5 Concluding remarks on the future perspectives of the field

The observational field of VHE gamma-ray astrophysics has been successfully driven in the last years by ground based imaging air Cherenkov telescopes. The “high energy frontier” of Astrophysics will be expanded by the results expected from the Fermi satellite. The all-sky sensitivity of the Fermi Large-Area-Telescope (LAT) will most likely lead to many interesting new discoveries and surprises. The inter-play of the Fermi-LAT detections from space and follow-up observations from ground will provide mutual benefits for the communities as well as certainly answer many questions as well as stimulate new ones.

While space-based observations of gamma-rays will be for a long time limited to the results obtained with Fermi (until maybe pair conversion telescopes will be deployed on the surface of the moon), ground based observatories will continue to be developed and constructed during the next decade(s). To my knowledge, besides Fermi, no further space-based gamma-ray telescope, operating in the GeV energy range, is planned. Consequently, ground based gamma-ray detection techniques will be the only available experimental approach to observe high energy gamma-rays after the termination of the Fermi mission.

The extensions of H.E.S.S. and MAGIC into phase II until 2009 will lower the energy threshold and improve existing sensitivity moderately. The next generation of ground based installations will become fully operational at the end of the next decade as envisaged in the AGIS<sup>16</sup>(Krawczynski et al. 2007) and CTA<sup>17</sup> (Hermann 2007) projects. These installations aim at an improvement in sensitivity by a factor of 10 and a widened reach in energy. At that time, the new ground based instruments including larger ( $> \text{km}^2$ ) installations like TenTen (Rowell et al. 2008) will explore new energy windows above  $\approx 10$  GeV as well as above 10 TeV.

However, there still remains a “blind spot”: the transient sky above 10 GeV will neither be explored very well with Fermi (limited photon rate) nor with ground based instruments of the current generation (limited field of view and energy threshold). New installations like HAWC (Sinnis & Hawc Collaboration 2005) will improve the situation in the energy range above a few 100 GeV. The lesson from the detection of fast transient events as seen from Cyg X-1 and PKS 2155-304 however is that we are

---

<sup>16</sup>Advanced gamma ray imaging system

<sup>17</sup>Cherenkov telescope array

very likely missing the fast variability of XRBs and AGN. Proper coverage of these objects requires instruments with a large field of view and an energy threshold well below 100 GeV.

## References

- A. Djannati-Atai et al. 2007, ArXiv e-prints, 0710.2247  
Abdo, A. A., Allen, B., Berley, D., et al. 2007a, ApJ, 658, L33  
— 2007b, ApJ, 664, L91  
Abdo, A. A., Allen, B. T., Berley, D., et al. 2007c, ApJ, 666, 361  
Acciari, V., Aliu, E., Beilicke, M., et al. 2008a, ArXiv e-prints, 808  
Acciari, V. A., Beilicke, M., Blaylock, G., et al. 2008b, ArXiv e-prints, 0802.1951  
Aharonian, F., Akhperjanian, A., Barrio, J., et al. 2001a, A&A, 370, 112  
Aharonian, F., Akhperjanian, A., Beilicke, M., et al. 2002a, A&A, 393, L37  
— 2002b, A&A, 393, 89  
— 2003a, A&A, 406, L9  
— 2003b, A&A, 403, L1  
— 2004a, ApJ, 614, 897  
— 2005a, A&A, 431, 197  
— 2006a, A&A, 454, 775  
Aharonian, F., Akhperjanian, A. G., Aye, K.-M., et al. 2004b, A&A, 425, L13  
— 2005b, Science, 307, 1938  
— 2005c, A&A, 435, L17  
— 2005d, A&A, 442, 1  
— 2005e, A&A, 436, L17  
— 2005f, A&A, 430, 865  
— 2005g, A&A, 432, L25  
Aharonian, F., Akhperjanian, A. G., Barres de Almeida, U., et al. 2007a, A&A, 473, L25  
— 2007b, A&A, 475, L9  
— 2008a, A&A, 477, 481  
— 2008b, A&A, 488, 219  
— 2008c, A&A, 477, 353  
Aharonian, F., Akhperjanian, A. G., Bazer-Bachi, A. R., & et al. 2006b, Science, 314, 1424  
Aharonian, F., Akhperjanian, A. G., Bazer-Bachi, A. R., et al. 2005h, A&A, 442, 177  
— 2005i, A&A, 442, 895  
— 2006c, A&A, 460, 743  
— 2006d, A&A, 449, 223  
— 2006e, Nature, 440, 1018  
— 2006f, A&A, 455, 461  
— 2006g, Nature, 439, 695  
— 2006h, A&A, 460, 365  
— 2006i, A&A, 448, L43  
— 2006j, Physical Review Letters, 97, 221102  
— 2006k, ApJ, 636, 777  
— 2007c, ApJ, 664, L71  
— 2007d, A&A, 467, 1075  
— 2007e, A&A, 470, 475  
— 2007f, ApJ, 661, 236  
— 2007g, A&A, 466, 543  
Aharonian, F., Khangulyan, D., & Costamante, L. 2008d, ArXiv e-prints, 0801.3198  
Aharonian, F. & Neronov, A. 2005, ApJ, 619, 306  
Aharonian, F. A., Akhperjanian, A. G., Barrio, J. A., et al. 2001b, A&A, 373, 292  
Aharonian, F. A., Akhperjanian, A. G., Bazer-Bachi, A. R., et al. 2005j, A&A, 442, L25  
— 2007h, A&A, 469, L1  
Aharonian, F. A. & Heinzlmann, G. 1998, Nuclear Physics B Proceedings Supplements, 60, 193  
Aharonian, F. A. et al. 2008e, ArXiv e-prints, 0801.3555  
Aielli, G. & The Argo-YBJ Collaboration. 2007, Nuclear Physics B Proceedings Supplements, 166, 96  
Albert, J., Aliu, E., Anderhub, H., Antoranz, P., et al. 2007a, ApJ, 667, L21  
Albert, J., Aliu, E., Anderhub, H., (The MAGIC Collaboration), & et al. 2008, Science, 320, 1752

Albert, J., Aliu, E., Anderhub, H., et al. 2006a, *ApJ*, 642, L119  
 —. 2006b, *ApJ*, 648, L105  
 —. 2006c, *ApJ*, 641, L9  
 —. 2006d, *ApJ*, 638, L101  
 —. 2006e, *ApJ*, 639, 761  
 —. 2006f, *Science*, 312, 1771  
 —. 2007b, *ApJ*, 669, 1143  
 —. 2007c, *ApJ*, 664, L87  
 —. 2007d, *ApJ*, 666, L17  
 —. 2007e, *ApJ*, 662, 892  
 —. 2007f, *A&A*, 474, 937  
 —. 2007g, *ApJ*, 669, 862  
 —. 2007h, *ApJ*, 665, L51  
 Albert, J. & for the MAGIC Collaboration. 2008, ArXiv e-prints, 0801.2391  
 Albert, J., for the MAGIC Collaboration, Ellis, J., Mavromatos, N. E., Nanopoulos, D. V., Sakharov, A. S., & Sarkisyan, E. K. G. 2007i, ArXiv e-prints, 0708.2889  
 Albinson, J. S., Tuffs, R. J., Swinbank, E., & Gull, S. F. 1986, *MNRAS*, 219, 427  
 Arons, J. & Tavani, M. 1994, *ApJS*, 90, 797  
 Aschenbach, B., Iyudin, A. F., & Schönfelder, V. 1999, *A&A*, 350, 997  
 Atkins, R., Benbow, W., Berley, D., et al. 2000, *ApJ*, 533, L119  
 —. 2004, *ApJ*, 608, 680  
 Atoyan, A. M., Aharonian, F. A., Tuffs, R. J., & Völk, H. J. 2000, *A&A*, 355, 211  
 Atwood, W. B., Bagagli, R., Baldini, L., et al. 2007, *Astroparticle Physics*, 28, 422  
 Baganoff, F. K., Maeda, Y., Morris, M., Bautz, M. W., Brandt, W. N., Cui, W., Doty, J. P., Feigelson, E. D., Garmire, G. P., Pravdo, S. H., Ricker, G. R., & Townsley, L. K. 2003, *ApJ*, 591, 891  
 Ballantyne, D. R., Melia, F., Liu, S., & Crocker, R. M. 2007, *ApJ*, 657, L13  
 Baltz, E. A., Briot, C., Salati, P., Taillet, R., & Silk, J. 2000, *PRD*, 61, 023514  
 Bamba, A., Yamazaki, R., & Hiraga, J. S. 2005, *ApJ*, 632, 294  
 Bamba, A., Yamazaki, R., Ueno, M., & Koyama, K. 2003, *ApJ*, 589, 827  
 Bednarek, W. 2007a, *MNRAS*, 382, 367  
 —. 2007b, *A&A*, 464, 259  
 Begelman, M. C., Fabian, A. C., & Rees, M. J. 2008, *MNRAS*, 384, L19  
 Berezhko, E. G., Ksenofontov, L. T., & Völk, H. J. 2003, *A&A*, 412, L11  
 Bettoni, D., Falomo, R., Fasano, G., & Govoni, F. 2003, *A&A*, 399, 869  
 Blanch, O. & Martinez, M. 2005a, *Astroparticle Physics*, 23, 598  
 —. 2005b, *Astroparticle Physics*, 23, 608  
 Blondin, J. M., Chevalier, R. A., & Frierson, D. M. 2001, *ApJ*, 563, 806  
 Bogovalov, S. V. & Aharonian, F. A. 2000, *MNRAS*, 313, 504  
 Bosch-Ramon, V., Romero, G. E., & Paredes, J. M. 2006, *A&A*, 447, 263  
 Bringmann, T., Bergström, L., & Edsjö, J. 2008, *Journal of High Energy Physics*, 1, 49  
 Cassam-Chenaï, G., Decourchelle, A., Ballet, J., Sauvageot, J.-L., Dubner, G., & Giacani, E. 2004, *A&A*, 427, 199  
 Celotti, A., Fabian, A. C., & Rees, M. J. 1998, *MNRAS*, 293, 239  
 Chadwick, P. M., Lyons, K., McComb, T. J. L., Orford, K. J., Osborne, J. L., Rayner, S. M., Shaw, S. E., Turver, K. E., & Wieczorek, G. J. 1999, *ApJ*, 513, 161  
 Claussen, M. J., Frail, D. A., Goss, W. M., & Gaume, R. A. 1997, *ApJ*, 489, 143  
 Costamante, L. & Ghisellini, G. 2002, *A&A*, 384, 56  
 Cowsik, R. & Sarkar, S. 1980, *MNRAS*, 191, 855  
 Crocker, R. M., Fatuzzo, M., Jokipii, J. R., Melia, F., & Volkas, R. R. 2005, *ApJ*, 622, 892  
 D. M. Gingrich, Boone, L. M., Bramel, D., et al. 2005, ArXiv Astrophysics e-prints  
 De Becker, M. 2007, *A&ARv*, 14, 171  
 Dhawan, V., Mioduszewski, A., & Rupen, M. 2006, in VI Microquasar Workshop: Microquasars and Beyond  
 Djannati-Ataï, A., Khelifi, B., Vorobiov, S., et al. 2002, *A&A*, 391, L25  
 Domainko, W., Benbow, W., Hinton, J. A., & others for the H. E. S. S. Collaboration. 2007, ArXiv e-prints, 708.1384  
 Domingo-Santamaría, E. & Torres, D. F. 2005, *A&A*, 444, 403  
 —. 2006, *A&A*, 448, 613  
 Drury, L. O., Aharonian, F. A., & Voelk, H. J. 1994, *A&A*, 287, 959  
 Dubus, G. 2006a, *A&A*, 451, 9  
 —. 2006b, *A&A*, 456, 801  
 Dwek, E. & Krennrich, F. 2005, *ApJ*, 618, 657  
 Ellis, J., Mavromatos, N. E., Nanopoulos, D. V., & Sakharov, A. S. 2003, *A&A*, 402, 409

- Ellis, J., Mavromatos, N. E., Nanopoulos, D. V., Sakharov, A. S., & Sarkisyan, E. K. G. 2006, *Astroparticle Physics*, 25, 402
- Erylkin, A. D. & Wolfendale, A. W. 2007, *Journal of Physics G Nuclear Physics*, 34, 1813
- Fermi, E. 1949, *Physical Review*, 75, 1169
- Ferreira, S. E. S. & de Jager, O. C. 2008, *A&A*, 478, 17
- Fontaine, G., Espigat, P., Ghesquiere, C., Schune, P., Baillon, P., Behr, L., Dudelzak, B., Eschstruth, P., Roy, P., Fabre, J., Meynadier, C., George, R., Kovacs, F., Pons, Y., Rivoal, M., & Socroun, T. 1990, *Nuclear Physics B Proceedings Supplements*, 14, 79
- Funk, S. 2007, *ApSS*, 309, 11
- Funk, S., Hinton, J. A., Moriguchi, Y., Aharonian, F. A., Fukui, Y., Hofmann, W., Horns, D., Pühlhofer, G., Reimer, O., Rowell, G., Terrier, R., Vink, J., & Wagner, S. J. 2007, *A&A*, 470, 249
- Gabici, S. & Aharonian, F. A. 2007, *ApJ*, 665, L131
- Gaensler, B. M., Schulz, N. S., Kaspi, V. M., Pivovarov, M. J., & Becker, W. E. 2003, *ApJ*, 588, 441
- Gaensler, B. M. & Slane, P. O. 2006, *ARA&A*, 44, 17
- Gaidos, J. A., Akerlof, C. W., Biller, S. D., et al. 1996, *Nature*, 383, 319
- Genzel, R., Schödel, R., Ott, T., Eckart, A., Alexander, T., Lacombe, F., Rouan, D., & Aschenbach, B. 2003, *Nature*, 425, 934
- Georganopoulos, M., Perlman, E. S., & Kazanas, D. 2005, *ApJ*, 634, L33
- Ghez, A. M., Salim, S., Hornstein, S. D., Tanner, A., Lu, J. R., Morris, M., Becklin, E. E., & Duchêne, G. 2005, *ApJ*, 620, 744
- Ginzburg, V. L. & Syrovatskii, S. I. 1964, *The Origin of Cosmic Rays (The Origin of Cosmic Rays, New York: Macmillan, 1964)*
- Gould, R. J. & Schröder, G. 1966, *Physical Review Letters*, 16, 252
- Grindlay, J. E., Helmken, H. F., Brown, R. H., Davis, J., & Allen, L. R. 1975, *ApJ*, 197, L9
- Hartman, R. C., Bertsch, D. L., Bloom, S. D., et al. 1999, *ApJS*, 123, 79
- Hartman, R. C., Bertsch, D. L., Fichtel, C. E., et al. 1992, *ApJ*, 385, L1
- Hartman, R. C., Böttcher, M., Aldering, G., et al. 2001, *ApJ*, 553, 683
- Hermann, G. 2007, *Astronomische Nachrichten*, 328, 600
- HESS Collaboration: F. Aharonian. 2008, *ArXiv e-prints*, 802
- Hillas, A. M. 2006, *ArXiv astro-ph/0607109*
- Hinton, J. 2007, *arXiv e-prints*, 0712.3352
- Hinton, J., Vivier, M., Bühler, R., Pühlhofer, G., & Wagner, S. 2007a, *ArXiv e-prints*, 0710.1537
- Hinton, J. A. & Aharonian, F. A. 2007, *ApJ*, 657, 302
- Hinton, J. A., Domaenko, W., & Pope, E. C. D. 2007b, *MNRAS*, 382, 466
- Hoppe, S., Lemoine-Goumard, M., & for the H. E. S. S. Collaboration. 2007, *ArXiv e-prints*, 0709.4103
- Horns, D. 2005, *Physics Letters B*, 607, 225
- Horns, D., Aharonian, F., Santangelo, A., Hoffmann, A. I. D., & Masterson, C. 2006, *A&A*, 451, L51
- Horns, D., Hoffmann, A. I. D., Santangelo, A., Aharonian, F. A., & Rowell, G. P. 2007, *A&A*, 469, L17
- Humensky, B. & VERITAAS Collaboration. 2008, in *American Institute of Physics Conference Series*, Vol. 888, to appear in *High Energy Gamma-Ray Astronomy*, ed. F. A. Aharonian & H. J. Völk, yyy-zzz
- Itoh, C., Enomoto, R., Yanagita, S., et al. 2007, *A&A*, 462, 67
- Kappes, A., Hinton, J., Stegmann, C., & Aharonian, F. A. 2007a, *ApJ*, 661, 1348
- . 2007b, *ApJ*, 656, 870
- Karle, A., Merck, M., Plaga, R., Arqueros, F., Hausteiner, V., Heinzlmann, G., Holl, I., Fonseca, V., Lorenz, E., Martinez, S., Matheis, V., Meyer, H., Mirzoyan, R., Prahl, J., Renker, D., Rozanska, M., & Samorski, M. 1995, *Astroparticle Physics*, 3, 321
- Kaspi, V. M., Roberts, M. S. E., & Harding, A. K. 2006, *Compact stellar X-ray sources*, 279
- Kawachi, A., Naito, T., Patterson, J. R., et al. 2004, *ApJ*, 607, 949
- Kawasaki, M., Ozaki, M., Nagase, F., Inoue, H., & Petre, R. 2005, *ApJ*, 631, 935
- Khangulyan, D., Aharonian, F., & Bosch-Ramon, V. 2008, *MNRAS*, 383, 467
- Khangulyan, D., Hnatic, S., Aharonian, F., & Bogovalov, S. 2007, *MNRAS*, 380, 320
- Kirk, J. G., Ball, L., & Skjaeraasen, O. 1999, *Astroparticle Physics*, 10, 31
- Konopelko, A., Atkins, R. W., Blaylock, G., et al. 2007, *ApJ*, 658, 1062
- Kosack, K., Badran, H. M., Bond, I. H., et al. 2004, *ApJ*, 608, L97
- Koyama, K., Kinugasa, K., Matsuzaki, K., Nishiuchi, M., Sugizaki, M., Torii, K., Yamauchi, S., & Aschenbach, B. 1997, *PASJ*, 49, L7

- Krawczynski, H., Buckley, J., Byrum, K., Dermer, C., Dingus, B., Falcone, A., Kaaret, P., Krennrich, F., Pohl, M., Vassiliev, V., Williams, D. A., & for the White Paper Team. 2007, ArXiv e-prints, 0709.0704
- Lang, M. J., Carter-Lewis, D. A., Fegan, D. J., et al. 2004, *A&A*, 423, 415
- Langston, G., Minter, A., D'Addario, L., Eberhardt, K., Koski, K., & Zuber, J. 2000, *AJ*, 119, 2801
- Le Bohec, S., Badran, H. M., Bond, I. H., et al. 2004, *ApJ*, 610, 156
- Lee, J.-J., Koo, B.-C., Yun, M. S., Stanimirović, S., Heiles, C., & Heyer, M. 2008, *AJ*, 135, 796
- Liu, S., Melia, F., Petrosian, V., & Fatuzzo, M. 2006, *ApJ*, 647, 1099
- Lorenz, E. 2007, *Journal of Physics Conference Series*, 60, 1
- Lucek, S. G. & Bell, A. R. 2000, *MNRAS*, 314, 65
- Maier, G. 2007, ArXiv e-prints, 0709.3661
- Manolakou, K., Horns, D., & Kirk, J. G. 2007, *A&A*, 474, 689
- Marleau, P., Alfonso, P., Chertok, M., et al. 2005, in *Cherenkov 2005*
- Mazin, D. & Raue, M. 2007, *A&A*, 471, 439
- Mizuno, A. & Fukui, Y. 2004, in *Astronomical Society of the Pacific Conference Series*, Vol. 317, *Milky Way Surveys: The Structure and Evolution of our Galaxy*, ed. D. Clemens, R. Shah, & T. Brainerd, 59–+
- Muno, M. P., Lu, J. R., Baganoff, F. K., Brandt, W. N., Garmire, G. P., Ghez, A. M., Hornstein, S. D., & Morris, M. R. 2005, *ApJ*, 633, 228
- Naumann-Godó, M. & H.E.S.S. Collaboration. 2008, in *American Institute of Physics Conference Series*, Vol. 888, to appear in *High Energy Gamma-Ray Astronomy*, ed. F. A. Aharonian & H. J. Völk, yyy–zzz
- Neronov, A. & Chernyakova, M. 2007, *ApSS*, 309, 253
- Neronov, A., Semikoz, D., & Sibiryakov, S. 2008, ArXiv e-prints, 806
- Nilsson, K., Pursimo, T., Sillanpää, A., Takalo, L. O., & Lindfors, E. 2008, *A&A*, 487, L29
- Padilla, L., Funk, B., Krawczynski, H., et al. 1998, *A&A*, 337, 43
- Paré, E., Balauge, B., Bazer-Bachi, R., et al. 2002, *Nuclear Instruments and Methods in Physics Research A*, 490, 71
- Paredes, J. M., Martí, J., Ishwara Chandra, C. H., & Bosch-Ramon, V. 2007, *ApJ*, 654, L135
- Pfrommer, C. & Enßlin, T. A. 2003, *A&A*, 407, L73
- . 2004, *A&A*, 413, 17
- Piner, B. G., Pant, N., & Edwards, P. G. 2008, ArXiv e-prints, 801
- Ptuskín, V. S. & Zirakashvili, V. N. 2005, *A&A*, 429, 755
- Punch, M., Akerlof, C. W., Cawley, M. F., et al. 1992, *Nature*, 358, 477
- Punch, M. f. t. H. c. 2007, in 30<sup>th</sup> ICRC, Merida Mexico, Vol. 1, *Proceedings of the 30th ICRC*
- Quataert, E. & Loeb, A. 2005, *ApJ*, 635, L45
- Quinn, J., Akerlof, C. W., Biller, S., et al. 1996, *ApJ*, 456, L83+
- Raue, M. & Mazin, D. 2008, ArXiv e-prints, 0802.0129
- Rauw, G., Manfroid, J., Gosset, E., Nazé, Y., Sana, H., De Becker, M., Foellmi, C., & Moffat, A. F. J. 2007, *A&A*, 463, 981
- Reed, J. E., Hester, J. J., Fabian, A. C., & Winkler, P. F. 1995, *ApJ*, 440, 706
- Reimer, A., Pohl, M., & Reimer, O. 2006, *ApJ*, 644, 1118
- Reimer, A., Protheroe, R. J., & Donea, A.-C. 2004, *A&A*, 419, 89
- Reimer, O., Aharonian, F., Hinton, J., Hofmann, W., Hoppe, S., Raue, M., & Reimer, A. 2007, ArXiv e-prints, 0710.3418
- Reynolds, S. P., Borkowski, K. J., Hwang, U., Hughes, J. P., Badenes, C., Laming, J. M., & Blondin, J. M. 2007, *ApJ*, 668, L135
- Reynoso, E. M. & Goss, W. M. 1999, *AJ*, 118, 926
- Rho, J. & Petre, R. 1998, *ApJ*, 503, L167+
- Ribó, M., Paredes, J. M., Moldón, J., Martí, J., & Massi, M. 2008, *A&A*, 481, 17
- Rowell, G. P., Stamatescu, V., Clay, R. W., Dawson, B. R., Protheroe, R. J., Smith, A. G. K., Thornton, G. J., & Wild, N. 2008, *Nuclear Instruments and Methods in Physics Research A*, 588, 48
- Samorski, M. & Stamm, W. 1983, *ApJ*, 268, L17
- Sarkar, S. 2002, *Modern Physics Letters A*, 17, 1025
- Schödel, R., Ott, T., Genzel, R., et al. 2002, *Nature*, 419, 694
- Schroedter, M., Badran, H. M., Buckley, J. H., et al. 2005, *ApJ*, 634, 947
- Schwarz, U. J., Goss, W. M., Kalberla, P. M., & Benaglia, P. 1995, *A&A*, 299, 193
- Sinnis, G. & Hawc Collaboration. 2005, in *American Institute of Physics Conference Series*, Vol. 745, *High Energy Gamma-Ray Astronomy*, ed. F. A. Aharonian, H. J. Völk, & D. Horns, 234–245



Slane, P., Hughes, J. P., Edgar, R. J., Plucinsky, P. P., Miyata, E., Tsunemi, H., & Aschenbach, B. 2001, *ApJ*, 548, 814  
Swordy, S. 2008, *The Astronomer's Telegram*, 1415, 1  
Teshima, M. 2008, *The Astronomer's Telegram*, 1491, 1  
Teshima, M., Prandini, E., Bock, R., et al. 2007, *ArXiv e-prints*, 0709.1475  
Teshima, M. & The MAGIC Collaboration. 2008, *The Astronomer's Telegram*, 1500, 1  
The H. E. S. S. Collaboration. 2007, *ArXiv e-prints*, 710  
Thompson, D. J., Bailes, M., Bertsch, D. L., et al. 1999, *ApJ*, 516, 297  
Thorstensen, J. R., Fesen, R. A., & van den Bergh, S. 2001, *AJ*, 122, 297  
Tsuchiya, K., Enomoto, R., Ksenofontov, L. T., et al. 2004, *ApJ*, 606, L115  
Uchiyama, Y., Aharonian, F. A., Tanaka, T., Takahashi, T., & Maeda, Y. 2007, *Nature*, 449, 576  
van Eldik, C., Bolz, O., Braun, I., Hermann, G., Hinton, J., & Hofmann, W. 2007, *ArXiv e-prints*, 0709.3729  
Velázquez, P. F., Dubner, G. M., Goss, W. M., & Green, A. J. 2002, *AJ*, 124, 2145  
Vink, J., Bleeker, J., van der Heyden, K., Bykov, A., Bamba, A., & Yamazaki, R. 2006, *ApJ*, 648, L33  
Voges, W., Aschenbach, B., Boller, T., et al. 2000, *VizieR Online Data Catalog*, 9029, 0  
Völk, H. J., Aharonian, F. A., & Breitschwerdt, D. 1996, *Space Science Reviews*, 75, 279  
Wagner, R. M. 2008, *MNRAS*, 385, 119  
Wang, Q. D., Lu, F. J., & Gotthelf, E. V. 2006, *MNRAS*, 367, 937  
Weekes, T. C. 1992, *Space Science Reviews*, 59, 315  
Winkler, P. F., Gupta, G., & Long, K. S. 2003, *ApJ*, 585, 324